



Investigation of Calcium Silicate Solubility in Various Aqueous Media

Viktoria Engqvist

Independent project • 15 credits
Swedish University of Agricultural Sciences, SLU
Faculty of Natural Resources of Agriculture Sciences
Department of Molecular Sciences
Molecular Sciences, 2025:07
Freestanding course in Chemistry
Uppsala, 2025



Investigation of Calcium Silicate Solubility in Various Aqueous Media

Viktorija Engqvist

Supervisor: Gulaim A. Seisenbaeva, Swedish University of Agricultural Sciences, Department of Molecular Sciences
Examiner: Anders Broberg, Swedish University of Agricultural Sciences, department of Molecular sciences

Credits: 15 credits
Level: G2E
Course title: Independent project in Chemistry
Course code: EX0878
Programme/education: Freestanding course in Chemistry
Course coordinating dept: Department of Molecular Sciences, SLU
Place of publication: Uppsala
Year of publication: 2025
Title of series: Molecular Sciences
Part number: 2025:07

Keywords: Solubility, Calcium silicate, NPK fertilizer, citric acid, bioavailability

Swedish University of Agricultural Sciences
Faculty of Natural Resources of Agriculture Sciences
Department of Molecular Sciences

Abstract

Calcium silicate (CaSiO_3) is a potential source of calcium and silicon for both agricultural and cosmetic applications, but its limited solubility in water poses a challenge for practical use. This study investigated dissolution behavior of calcium silicate in different aqueous environments: pure water, NPK fertilizer solution, and citric acid-containing systems. Solubility was assessed through measurements of total and free calcium concentrations using ICP-OES and ion-selective electrode (ISE), along with pH, TGA, SEM-EDS, and XRD analyses to characterize solid residues.

Results confirmed very low solubility in water, with a sharp increase in pH and rapid saturation of free Ca^{2+} ions. In NPK solutions, calcium silicate partially dissolved but showed signs of secondary precipitation, likely due to interactions with phosphate. The addition of citric acid significantly improved calcium ion availability, particularly at a concentration of 0.035%, which maintained higher levels of free Ca^{2+} without excessive complexation. Solid-state analysis showed that crystalline residues remained at higher dosages, while low concentrations favored amorphous or partially reacted phases.

Overall, the findings suggest that citric acid could be an effective additive to improve calcium silicate solubility and bioavailability in nutrient formulations but needs further investigation and also comparison with other co-solvents. This work provides insight into optimizing calcium silicate use in controlled-release systems.

Table of contents

List of figures	8
1. Introduction	10
1.1 Aim	10
2. Theoretical background	11
2.1 Solubility Calcium metasilicate.....	11
2.2 Lattice and hydration enthalpy.....	12
2.3 pH.....	13
2.4 Co-solvents	13
2.4.1 Citric acid as a co-solvent.....	14
2.5 NPK.....	15
2.5.1 Nitrogen (N)	15
2.5.2 Phosphorus (P).....	15
2.5.3 Potassium	15
2.6 Silicon effect on plants	16
2.7 Practical implications of using NPK and silicon together	16
2.8 Citric Acid as an Organic Acid and Chelating Agent.....	17
2.9 Technical instrumental	17
2.9.1 Ion Selective Electrode (ISE).....	17
2.9.2 pH – measuring	18
2.9.3 Inductively Coupled Plasma Optical Emission Spectroscopy (ICP-OES)	18
2.9.4 Thermogravimetric analysis (TGA)	19
2.9.5 Scanning Electron Microscope (SEM-EDS)	19
2.9.6 X-ray diffractometer (XRD)	20
3. Experimental	22
3.1 Solubility H ₂ O	22
3.2 Solubility in co-solvents.....	22
3.3 Solubility in NPK solution	22
3.4 Solubility in NPK and Citric Acid	22
3.5 pH meter	23
3.6 Ion Selective Electrode	23
3.7 Sample analysis ICP – OES	23
3.8 Sample analysis TGA	25
3.9 Sample analysis SEM-EDS and XRD.....	25
4. Results and Discussion	26
4.1 Solubility in H ₂ O	26
4.2 Solubility in co-solvents.....	29
4.3 Solubility in NPK solution	34

4.3.1	TGA.....	36
4.3.2	SEM-EDS.....	39
4.3.3	XRD	44
4.4	Solubility in NPK solutions containing citric acid.....	45
4.4.1	TGA.....	48
4.4.2	SEM-EDS.....	49
4.4.3	XRD	50
5.	Conclusions.....	52
	References	54

List of figures

Figure 1. Structure of Calcium metasilicate. Figure by Peter Thiessen et al. Journal of Physical Chemistry C 2015, 119(19):150420120117006	11
Figure 2. Structure of citric acid. Figure made in Chemdraw.....	14
Figure 3. Simplified representation of calcium citrate complex. Figure made in Chemdraw.	14
Figure 4. Example of picture Scanning Electron Microscope. Figure taken from a sample in this thesis.	20
Figure 5. Calibration curve from ICP-OES	24
Figure 6. pH trend as a function of calcium silicate dosage.....	26
Figure 7. ICP measurements of Ca and Si in solution (mg/dL).....	27
Figure 8. . Converted ICP concentrations (mmol/dL) of Ca and Si.....	27
Figure 9. ISE measurements of free Ca ²⁺ (mmol/dL) and pH.....	28
Figure 10. Comparison of total Ca (ICP) vs. free Ca ²⁺ (ISE)	29
Figure 11. pH trend with citric acid 0,07%.....	30
Figure 12. . pH trend with citric acid 0,035%	30
Figure 13. . ICP Analysis Ca and Si, citric acid 0,07%	31
Figure 14. . ICP Analysis Ca and Si, citric acid 0,035%	31
Figure 15. ICP results converted to mmol/dL, citric acid 0,07%	32
Figure 16. ICP results converted to mmol/dL, citric acid 0,035%	32
Figure 17. ISE measurements of free Ca ²⁺ , solution with citric acid 0,07%	33
Figure 18. ISE measurements of free Ca ²⁺ , solution with citric acid 0,035%	33
Figure 19 ICP and ISE comparison Ca ²⁺ concentration.....	34
Figure 20. pH in NPK Solution with Calcium Silicate	35
Figure 21. Free Ca ²⁺ Activity Measured by ISE	35
Figure 22. Comparison of ISE and ICP.....	36
Figure 23. The TGA curve of sample NPK + 0.001 g CaSiO ₃	37
Figure 24. TGA curve of sample NPK + 0.01 g CaSiO ₃	38
Figure 25. TGA curve on sample containing NPK + 1 g CaSiO ₃	39
Figure 26. SEM image of 0.001 g CaSiO ₃ sample.....	40

Figure 27. Sum spectrum map of 0.001 g CaSiO ₃ sample	40
Figure 28. SEM image of 0.01 g CaSiO ₃ sample.....	42
Figure 29. Sum spectrum map of 0.01 g CaSiO ₃ sample	42
Figure 30. SEM image of 1 g CaSiO ₃ sample.....	43
Figure 31. Map Sum Spectrum of 1 g CaSiO ₃ sample	43
Figure 32. XRD pattern of 0,001 g CaSiO ₃ sample.....	44
Figure 33. XRD pattern of 0,01g CaSiO ₃ sample	45
Figure 34. XRD pattern of 1 g CaSiO ₃ sample.....	45
Figure 35 and 36. pH development in NPK + citric acid + CaSiO ₃ systems.....	46
Figure 37. ISE measurements of free Ca ²⁺ in 0.07% citric acid.....	46
Figure 38. ISE measurements of free Ca ²⁺ in 0.07% citric acid.....	47
Figure 39. Comparison of ISE values between 0.035% and 0.07% citric acid	47
Figure 40. CaSiO ₃ _NPK_Citric acid_	49
Figure 41. SEM image of NPK+Citric acid+CaSiO ₃	49
Figure 42. EDS analysis of elemental composition.....	50
Figure 43. XRD diffractogram of NPK+Citric acid+ CaSiO ₃	51

1. Introduction

The solubility of calcium silicate (CaSiO_3), is widely used in the industrial field but it remains poorly understood in complex aqueous systems. While its use in ceramics and cement is well established, the potential for calcium silicate as a sustainable nutrient source in for both humans and plants needs further investigation. In particular, its limited solubility in pure water, coupled with its reactivity in acidic or nutrient-rich environments, raises questions about its suitability in different liquid solutions for example water based formulations as an application for the human body and as a fertilizer formulation for plants.

Both calcium and silicon are known for their beneficial properties when it comes to the regeneration and strengthening of proteins involved in the structure of our skin, hair, and nails. But it is also known that calcium silicate can contribute these essential elements to plant nutrition. However, factors such as pH, co-solvent presence, and nutrient interactions may influence its dissolution behavior and nutrient availability. Existing literature suggests that weak acids, like citric acid, could enhance solubility through both pH modulation and chelation, but systematic data under agriculturally relevant conditions are lacking.

This project investigates how calcium silicate behaves in various aqueous media, with a focus on water, NPK fertilizer solutions, and citric acid systems. By quantifying solubility and calcium ion activity, the study aims to clarify under which conditions CaSiO_3 can effectively release bioavailable nutrients for both human and plants.

1.1 Aim

The aim of this project is to investigate the solubility of calcium silicate (CaSiO_3) under different aqueous conditions, including water, NPK fertilizer solutions, and citric acid-containing media.

2. Theoretical background

2.1 Solubility Calcium metasilicate

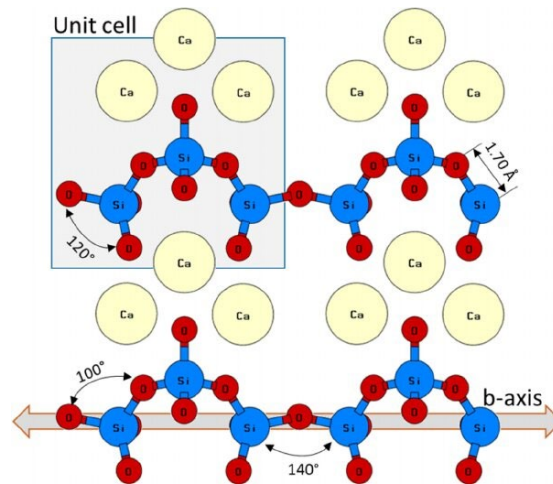
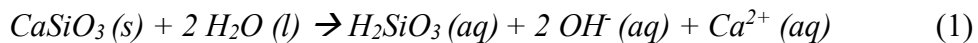


Figure 1. Structure of Calcium metasilicate. Figure by Peter Thiessen et al. *Journal of Physical Chemistry C* 2015, 119(19):150420120117006

Calcium metasilicate, commonly occurring in nature as the mineral wollastonite, a polymeric chain silicate of so called pyroxene class, is a compound traditionally used in ceramics and cement. It is typically found as a white, odorless powder with a solubility of approximately 0.01w% in water. Naturally occurring calcium silicate has a theoretical composition of 48.3% calcium oxide (CaO) and 51.7% silicon dioxide (SiO₂). Despite this, due to its structural characteristics (see Figure 1), it is conventionally represented as CaSiO₃ in chemical reactions (National Center for Biotechnology Information, n.d.). When exposed to water, calcium silicate is believed to undergo a two-step hydrolysis process. The initial hydrolysis yields polymeric metasilicic acid and hydroxide ions, resulting in a pH range of 8–10.



Second hydrolysis resulting in de-polymerisation producing orthosilicic acid:

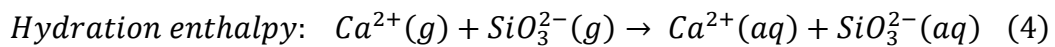
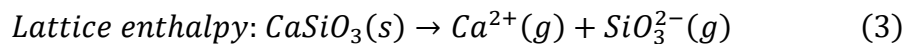


2.2 Lattice and hydration enthalpy

Solubility of salts influenced by multiple factors and is a complex phenomenon. From a thermodynamic perspective, the solubility of a salt in water is primarily determined by two opposing enthalpic contributions: lattice enthalpy and hydration enthalpy.

Lattice enthalpy ($\Delta_{\text{latt}}H^\circ$) is the energy released when one mole of an ionic compound is formed from its gaseous ions, or opposite, the energy required to break one mole of an ionic solid into its gaseous ions. Positive lattice enthalpy is the energy required to separate the ions in an ionic solid into gaseous ions (see Reaction 1). It reflects the strength of the electrostatic forces between ions within the solid lattice; a higher lattice enthalpy corresponds to stronger ionic interactions. This enthalpy increases with greater ionic charge, smaller ionic radius, and a more tightly packed crystal structure—all of which are characteristic of calcium silicate (Aylward and Findlay, 2008; Weller et al., 2018; Sketchfab, 2021). In order for a salt to dissolve, its lattice structure must first be disrupted (Weller et al., 2018).

Once dissociated in an aqueous environment, the individual ions interact with surrounding water molecules. The energy released when one mole of gaseous ions dissolves in water to form hydrated (aqueous) ions and is defined by hydration enthalpy ($\Delta_{\text{hyd}}H^\circ$) (see Reaction 2). A more negative hydration enthalpy indicates a greater release of energy during solvation, making the dissolution process more thermodynamically favorable. Hydration enthalpy increases with decreasing ionic size and increasing polarity of the ions (Weller et al., 2018).



Hess's law (see Equation 1) describes the relation between lattice enthalpy and hydration enthalpy. The relationship between lattice enthalpy and hydration enthalpy is described by Hess's law (see Equation 1). The difference between these two enthalpic values yields the enthalpy of solution ($\Delta_{\text{sol}}H^\circ$), which serves as an indirect indicator of the solubility of an ionic compound.

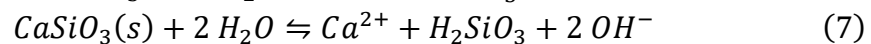
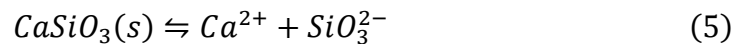
$$\Delta_{\text{sol}}H^\circ = \Delta_{\text{hyd}}H^\circ - \Delta_{\text{Latt}}H^\circ \quad \text{Eq. 1}$$

For calcium metasilicate (CaSiO_3) the lattice enthalpy is highly positive, reflecting strong ionic interactions within the crystal structure. In contrast, the absolute value of its hydration enthalpy is relatively low, primarily due to the large size and low polarity of the polymeric SiO_3^{2-} anion. This imbalance results in a positive enthalpy of solution, indicating that the dissolution of CaSiO_3 in water is thermodynamically unfavorable. This explains its low solubility of approximately 0.01w%, as reported in previous studies (Weller et al., 2018; Wypych, 2021; Sketchfab, 2021).

2.3 pH

The pH of the surrounding solution can influence the solubility of salts. In general, salts that produce anions which are conjugate bases of weak acids tend to exhibit increased solubility at lower pH levels. This is because a decrease in pH corresponds to a higher concentration of hydrogen ions (H^+), which can interact with and protonate the anions, thereby shifting the dissolution equilibrium (Schka and Sadowski, 2024). According to Le Chatelier's principle, when a system at equilibrium experiences a disturbance—such as a change in temperature, pressure, or concentration—a counteracting response occurs to re-establish equilibrium (Norwich, 2010). In this context, the continuous removal of anions through protonation drives the equilibrium toward increased salt dissolution.

Calcium silicate (CaSiO_3), dissociates into calcium ions and silicate ions of varying hydration states (see Reactions 5,6 and 7). The silicate ion acts as the conjugate base of metasilicic acid (H_2SiO_3), a weak acid that is more soluble in water than calcium silicate itself. When the pH is lowered, the higher concentration of hydrogen ions promotes the conversion of silicate ions into metasilicic acid.



2.4 Co-solvents

Due to calcium silicate low solubility in aqueous media, addition of co-solvent has been investigated for investigation on enhancing the solubility.

2.4.1 Citric acid as a co-solvent

Citric acid is a water-soluble, colorless crystalline compound with low toxicity. It occurs naturally in many plants and certain microorganisms due to its central role in biological oxidation pathways.

The molecule contains three carboxylic acid groups, with dissociation constants $pK_{a1} = 3.1$, $pK_{a2} = 4.8$, and $pK_{a3} = 6.4$ (see Figure 3), which makes it an effective buffering agent within the pH range of approximately 3.0 to 6.2. Notably, citric acid can form stable salts with a variety of metal ions. When calcium is present, it reacts to form calcium citrate—a compound with limited solubility (0.095 g/100 mL) (Goldberg and Rokem, 2009; The Protein Man, 2014; PubChem, 2025).

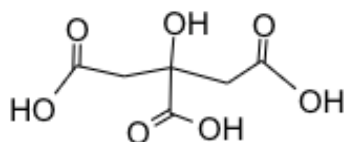


Figure 2. Structure of citric acid. Figure made in Chemdraw.

Due to its ability to interact with calcium to form calcium citrate and its tendency to lower the solution's pH, citric acid can act as a dissolving agent for calcium-containing complexes. Citric acid's ability to dissolve calcium silicate complexes at physiological pH has not yet been investigated (National Cancer Institute, 2011; Fiume et al., 2014; Lim et al., 2020; Drukteinis et al., 2024).

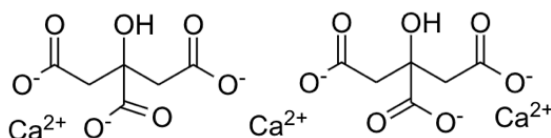


Figure 3. Simplified representation of calcium citrate complex. Figure made in Chemdraw.

2.5 NPK

The use of complex fertilizers such as NPK to intensify the growth of plants is widespread. Nitrogen (N), potassium (K) and phosphorus (P) are macronutrients, and therefore are consumed in higher amounts in plants. These nutrients are often present in various chemical compounds, such as ammonium nitrate (for nitrogen), superphosphate (for phosphorus), and potassium chloride (for potassium). Combination of these chemical substances provide NPK with high solubility leading to enhanced availability of the nutrients. The essential effects of NPK elements in an NPK fertilizer are:

2.5.1 Nitrogen (N)

Nitrogen is the main component in the earth's atmosphere and is the most abundant mineral required by the plant. It acts as an important determinant of plant growth (Rinsi and Espen, 2015).

Nitrogen is essential as it plays a crucial role in chlorophyll, the molecule that enables plants to harness energy from sunlight and convert water and carbon dioxide into sugars (a process known as photosynthesis). Additionally, nitrogen is a key element in nucleic acids and proteins (Nguyen et al., 2015). Nitrogen is a component in energy transfer compounds, such as ATP (adenosine triphosphate). ATP allows cells to conserve and use the energy released in metabolism.

2.5.2 Phosphorus (P)

Phosphorus is another essential element and is required for the development and growth of plants (Alori, Glick and Babalola, 2017). Phosphorus is an important component in plants DNA and RNA. Phosphorus is also important for the development of roots, flowers, seeds, fruits, energy for the plant and for the sorption of other elements including N (Khan et al., 2023).

2.5.3 Potassium

Potassium is a vital macronutrient that supports various physiological and biochemical processes in plants. It plays significant roles in plants like osmoregulation, membrane potential regulation, cotransport of sugars, stress adaption and growth (Johnson et al., 2022).

2.6 Silicon effect on plants

Silicon is one of the most commonly occurring chemical element in nature. Recent research has proved that supplementary application of silicon positively influences many aspects of plant growth.

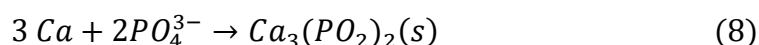
It is well known that silicon is involved in plant tolerance against many stress factors: it increases manganese and heavy metal tolerance as well as resistance against pathogens, like fungi or herbivorous insects. It helps plants survive in the conditions of water shortage (Dębicz and Wróblewska, 2012). Silicon deposition of silica in shoots and leaf epidermis, also known as the mechanical barrier hypothesis, enhances the plant's mechanical strength and protective layer (Tubana, Babu and Datnoff, 2016).

2.7 Practical implications of using NPK and silicon together

The combined application of NPK fertilizers and silicon supplements presents several practical benefits for modern agriculture, particularly in regions challenged by soil degradation, drought, or nutrient imbalances.

Silicon not only contributes to enhanced crop yield but also supports sustainable farming practices by decreasing the reliance on chemical fertilizers and pesticides. Studies have demonstrated that silicon can reduce the occurrence of plant diseases such as rusts and blights by reinforcing the plant's natural defense systems (Guntzer, Keller, & Meunier, 2012; Fauteux et al., 2005). Consequently, the integration of NPK and silicon has emerged as a promising strategy for improving crop productivity while advancing environmental sustainability.

When silicon is introduced in the form of calcium silicate into an NPK solution, chemical interactions may affect nutrient solubility. In particular, calcium ions (Ca^{2+}) from calcium silicate can react with phosphate ions (PO_4^{3-}) from the NPK solution, potentially leading to the formation of insoluble calcium phosphate precipitates (see reaction 7). This reduces the amount of phosphorus available in solution and may limit its immediate uptake by plants. In contrast, potassium (K^+) and nitrogen, typically present as nitrate (NO_3^-) or ammonium (NH_4^+), generally remain soluble and are less affected by the presence of calcium silicate. Therefore, while the use of calcium silicate in combination with NPK can offer long-term agronomic benefits, it is important to consider possible precipitation reactions—particularly in liquid formulations or hydroponic systems—to avoid reduced phosphorus availability.



Optimizing formulation parameters—such as concentration, pH, and timing of application—can help mitigate these interactions and ensure balanced nutrient availability.

2.8 Citric Acid as an Organic Acid and Chelating Agent

Through chelation, citric acid effectively "shields" calcium from reacting with phosphate, thereby maintaining phosphate solubility in the solution. The formation of calcium-citrate complexes reduces the free Ca^{2+} ion concentration, minimizing the risk of calcium phosphate precipitation and improving the overall nutrient balance in the system (Wei, Chen and Xu, 2010).

As a result, citric acid helps maintain both calcium and phosphate in soluble forms, which is particularly beneficial in hydroponic systems and soil amendments where nutrient availability is critical. The dynamic balance between these ions is influenced by pH, concentration, and the presence of competing ligands, but under controlled conditions, citric acid effectively shifts the equilibrium toward greater nutrient solubility and uptake efficiency.

It is well documented that calcium phosphate typically precipitates first in an amorphous form before crystallizing into more thermodynamically stable structures such as hydroxyapatite or tricalcium phosphate under appropriate conditions (Carino *et al.*, 2018).

2.9 Technical instrumental

2.9.1 Ion Selective Electrode (ISE)

The solubility of a salt refers to the maximum amount that can dissolve completely in a given volume of solvent. When a salt dissolves in water, it separates into its constituent cations and anions.

To estimate solubility, one can measure the concentration of one of these ions in solution—commonly using an ion-selective electrode (ISE).

An ISE functions through a selective membrane that ideally allows only a specific ion to pass. At equilibrium, a voltage difference is established across the membrane due to ion activity, which the electrode registers as an electrical potential. This potential is then related to the ion concentration via the Nernst

equation (Equation 2), which describes a logarithmic relationship between potential and concentration:

$$E = E^{\circ} - \frac{RT}{nF} \ln Q \quad \text{Eq. 2}$$

Where E is the measured potential. E° is a constant characteristic of the electrode, R is the gas constant ($8.314 \text{ J}\cdot\text{mol}^{-1}\cdot\text{K}^{-1}$), T is the temperature in Kelvin, F is the Faraday constant ($96,500 \text{ C/mol}$), n is the ion's charge, and Q represents the ion's concentration (Harris & Lucy, 2020).

2.9.2 pH – measuring

The pH of a solution is determined using a pH meter, which operates by detecting the electrical potential that correlates with the hydrogen ion concentration in the solution. Prior to use, the device is calibrated using standard buffer solutions, typically at pH values of 4, 7, and 10 [AD1]. This allows the hydrogen ion activity to be translated into a numerical value on the pH scale, which ranges from 0 to 14.

A standard pH meter setup includes a glass electrode, a reference electrode, and a voltmeter to register the voltage difference between the two electrodes. The glass electrode features a sensitive membrane that selectively interacts with hydrogen and alkali ions. Meanwhile, the reference electrode often consists of a silver/silver chloride element immersed in a potassium chloride solution and connected via a platinum wire (Galster, 1991).

In this study, the pH meter used was the HI1131B from HANNA Instruments. Unlike typical designs, this model integrates both the sensing and reference components into a single probe, known as a combination electrode. It uses a double junction system that minimizes sample contamination by isolating the internal 3.5 M potassium chloride solution from direct contact with the test medium. (Galster, 1991).

2.9.3 Inductively Coupled Plasma Optical Emission Spectroscopy (ICP-OES)

Inductively Coupled Plasma Optical Emission Spectroscopy (ICP-OES) is an analytical technique based on the use of a high-temperature plasma, generated by radiofrequency energy, to excite atoms within a sample.

When the sample is introduced into the plasma, it is subjected to extreme temperatures that cause atomization and ionization. As the excited atoms relax back to lower energy states, they emit light at specific wavelengths characteristic of each element. This emitted light is then separated by a spectrometer and detected using either a photomultiplier tube or a charge-coupled device (CCD). By examining the intensity and position of these wavelengths, the system can accurately determine the elemental composition of the sample (Boss & Fredeen, 2004).

2.9.4 Thermogravimetric analysis (TGA)

Thermogravimetric analysis (TGA) is an analytical technique used to measure the change in mass of a material as a function of temperature or time under a controlled atmosphere. It is particularly useful for studying thermal stability, composition, and the thermal decomposition behavior of materials.

In a typical TGA experiment, a sample is placed in a high-precision balance located within a furnace. As the temperature increases, changes in the sample's mass are continuously recorded. These changes can be linked to physical events such as moisture evaporation or to chemical processes such as decomposition, oxidation, or phase transitions.

TGA is widely applied in material science, chemistry, and environmental studies. In fertilizer research, it allows for the evaluation of how components such as ammonium salts, phosphates, or silicate additives decompose or volatilize upon heating. Characteristic weight loss steps can be assigned to distinct processes, for example, water release below 150°C, decomposition of organic matter or nitrate-based compounds between 200–400°C, or breakdown of more stable mineral components at higher temperatures.

The results are often presented as a thermogram: a curve showing weight percentage versus temperature, sometimes supplemented with a derivative curve (DTG) indicating the rate of mass loss. By interpreting these curves, researchers can deduce the composition and stability of complex mixtures, understand reaction pathways, and assess the effectiveness of additives. (Alvarenga *et al.*, 2012).

2.9.5 Scanning Electron Microscope (SEM-EDS)

Scanning Electron Microscope (SEM)—the most widely used form of electron microscopy. In SEM, a focused electron beam is scanned across the surface of the sample. As electrons interact with the sample's surface, they generate various

signals which are detected and used to construct a high-resolution image of the sample's topography and morphology.

When the SEM is equipped with an Energy Dispersive X-ray Spectroscopy (EDS or EDX) detector, it becomes possible to analyze the elemental composition of the sample, specifically for elements with atomic numbers greater than 10. When an incoming high-energy electron ejects an inner-shell electron from an atom in the sample, a vacancy is created. An electron from an outer shell then falls into the vacancy, and the excess energy is released as an X-ray photon. Each element emits X-rays at characteristic energy levels, making it possible to identify the chemical elements presenting the sample with a high degree of accuracy.

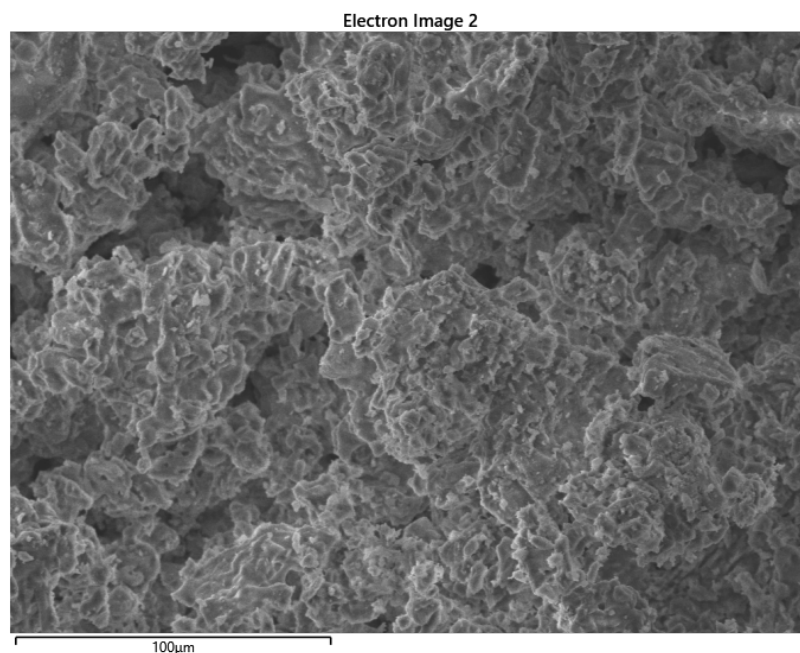


Figure 4. Example of picture Scanning Electron Microscope. Figure taken from a sample in this thesis.

2.9.6 X-ray diffractometer

X-ray diffraction (XRD) is a widely used analytical method for determining and characterizing unknown crystalline substances. In crystalline materials, atoms or molecules are arranged in a precise and repeating three-dimensional pattern. This organized structure results in a state of minimized internal energy and maximized intermolecular attraction.

The fundamental structural component of a crystal is known as the unit cell—a small, repeating block that builds up the entire crystal lattice. To begin identifying an unknown mineral, one typically starts by determining the dimensions and geometry of its unit cell. If the mineral's crystals are well-formed, X-ray

diffraction can be used to accurately measure the lengths and angles of the unit cell's edges.

Powder X-ray diffraction (PXRD) is a technique often used to analyze and identify samples that may contain multiple crystalline phases. The X-rays utilized in the method are produced in a sealed tube, where a tungsten filament emits electrons when heated. These electrons are then accelerated by an applied voltage and directed toward a metal target—typically copper or molybdenum—resulting in the emission of characteristic $K\alpha$ radiation, with wavelengths of 1.5418 Å for copper and 0.7107 Å for molybdenum.

To prepare the sample, the mineral is finely ground into a powder, to ensure that the crystallites are randomly oriented. This randomness increases the probability that the crystal lattice planes will align in all directions. When the X-ray beam is directed at the powdered sample, the X-rays are diffracted by the crystal structures. Each set of lattice planes can scatter the radiation, but for a visible diffraction peak to occur, the scattered waves must constructively interfere. Every crystalline material exhibits a distinct X-ray powder diffraction pattern, which can serve as a "fingerprint" for its identification.

In the final step of the identification process, this unique pattern is compared with reference data in a database to find matches with known substances (Atkins, 1996).

3. Experimental

The following section outlines the experimental methodology used in this project. Experiments were conducted using calcium silicate in different solvent systems—including pure water, NPK solution, and citric acid mixtures—to evaluate solubility and ion availability. Each setup was repeated in triplicates to ensure reproducibility and account for potential variation in ion measurements.

3.1 Solubility H₂O

Samples with 100 ml water with different concentrations (0.01 g, 0.02 g, 0.03 g, 0.04 g, 0.05 g, 0,1 g, 0,2 g) CaSiO₃ (s) respectively was prepared. The samples were stirred for 5 minutes on a magnetic stirrer and 10 ml was transferred to test tube for ICP analysis and 90 ml was transferred to test tube for pH analysis and analysis with ISE.

3.2 Solubility in co-solvents

To examine how the addition of a co-solvent affects solubility, varying amounts of CaSiO₃ (0.01 g, 0.02 g, 0.04 g, 0,05 g, 0,1 g, 0,2 g) were added to 100 ml of citric acid solutions at concentrations of 0.07% and 0.035%. The mixtures were stirred magnetically for 5 minutes. Afterwards, each sample was collected for ICP analysis, pH measurement and ion-selective electrode (ISE) analysis.

3.3 Solubility in NPK solution

NPK solutions dissolved in water, with varying amounts of calcium silicate (0.01 g, 0.02 g, 0.04 g, 0,05 g, 0,1 g, 0,2 g) added to the mixture were prepared. The samples were stirred magnetically for 5 minutes to ensure thorough dispersion. After mixing, each sample was collected for ICP analysis to determine elemental concentrations, pH measurement and ion-selective electrode (ISE) analysis. This procedure was designed to investigate the solubility of calcium silicate in aqueous NPK solutions with the concentration 0,38 g/L.

3.4 Solubility in NPK and Citric Acid

The same quantities of calcium silicate were added to NPK solutions with thw concentration 0,38 g/L, that also contained citric acid at two different concentrations (0.07% and 0.035%). The samples were stirred for 5 minutes to

achieve homogeneity before being divided for ICP, pH, and ISE analyses as described previously. This allowed for a comparative study on the effect of citric acid on the interaction between calcium silicate and NPK in solution.

3.5 pH meter

pH measurements were carried out using a HI1131B electrode from HANNA Instruments, with HI7082S (3.5 M KCl) employed as the reference electrolyte fill solution. The instrument was calibrated using a three-point method with standard buffer solutions at pH 4.01 (HI7004C), pH 7.01 (HI7007C), and pH 10.01 (HI7010C). To ensure accurate readings, the electrode was rinsed with deionized water between measurements and stored in HI70300L storage solution when not in use.

3.6 Ion Selective Electrode

A calcium-selective electrode (model HI4104, HANNA Instruments) was employed for free calcium ion measurements. This combination electrode was filled with HI7082S (3.5 M KCl) as the internal reference solution. Calibration was carried out using a three-point method with standard calcium solutions of 0.01 M, 0.001 M, and 0.0001 M, which were prepared through serial dilution from a 0.10 M stock solution (HI4004-01). To maintain consistent ionic strength across all standards and samples, 2 mL of ionic strength adjuster (HI4004-00) was added per 100 mL of solution. Between measurements, the electrode was rinsed with deionized water and stored in HI4004-45 storage solution to preserve functionality.

3.7 Sample analysis ICP – OES

Prior to the ICP-OES measurements, a calibration curve was established using standard solutions containing known concentrations of calcium and silicon in water, ranging from 0.1 to 10 mg/L.

The resulting curve demonstrated excellent linearity, with a correlation coefficient (R^2) greater than 0.99, as illustrated in Figure 5.

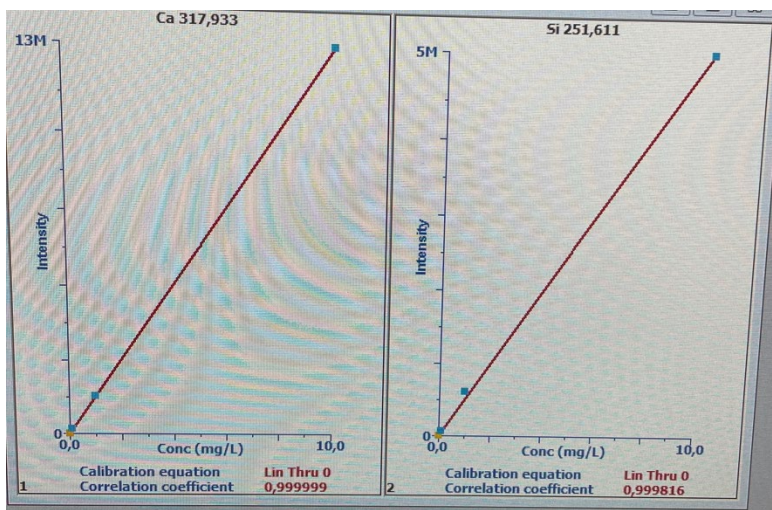


Figure 5. Calibration curve from ICP-OES

The experimental samples from the NPK and calcium silicate tests were prepared by diluting them with deionized water at a 1:10 ratio to ensure compatibility with the instrument. Each sample was subsequently filtered using a Whatman Puradisc 45 filter equipped with a 0.45 μm polyethersulfone (PES) membrane. Filtration was carried out to eliminate particulate matter and prevent clogging of the instrument, thereby improving measurement accuracy and minimizing analytical interferences. Since ICP-OES only detects dissolved elements, the filtration step does not affect the sample's ionic content, flow rate, or permeability.

Concentration analysis of the samples was performed by using ICP-OES with the settings shown in table 1.

Table 1. ICP-OES settings

Model	Avio 200
Sample flow	1 mL/min
Number of replicates	3
Pump speed	15 RPM
Analyzing time	30 s
Rinse time	120 s
Number of standards	3 (0,1, 1, 10 /mg/L)

Analytes: Ca (317,938), Si (251,615)

3.8 Sample analysis TGA

For the thermogravimetric measurements, samples were first prepared by drying them for 48 hours to remove any moisture content. The samples that was analyzed was only NPK solutions, containing 0,001g, 0,01g and 1g. One test with NPK solutions containg citric acid 0,07% and 0,01 g of calcium silicate. The material, originally in powder form, was ground using a mortar to achieve a fine and homogeneous powder before analysis. The TGA was conducted under an oxygen atmosphere with a temperature range from 25 °C to 900 °C with a rate of 5°C/min and a constant gas flow rate of 2 ml/min. This setup allowed for precise monitoring of the sample's weight changes as a function of temperature under oxidative conditions.

3.9 Sample analysis SEM-EDS and XRD

The residues remaining after the TGA analysis were further examined using scanning electron microscopy coupled with energy-dispersive X-ray spectroscopy (SEM-EDS) and X-ray powder diffraction (XRD) to characterize their morphology and phase composition.

4. Results and Discussion

4.1 Solubility in H₂O

The solubility of calcium silicate (CaSiO₃) in water was investigated by preparing aqueous solutions with increasing concentrations ranging from 0.01 to 0.5 mg/dL. The experiment involved measuring pH, total calcium and silicon content using inductively coupled plasma (ICP), and free calcium ion activity via ion-selective electrode (ISE). The data were also converted into molar concentrations for better comparison.

The pH of the solution increased sharply with added calcium silicate, rising from 7.6 to over 9.4 (Figure 6). This rapid pH shift suggests that hydroxide ions are released into solution during the dissolution of CaSiO₃, likely through hydrolysis of silicate. The curve levels off around 0.2–0.5 mg/dL, indicating a buffering or equilibrium-limited environment where further pH change is minimal despite increased solid addition.

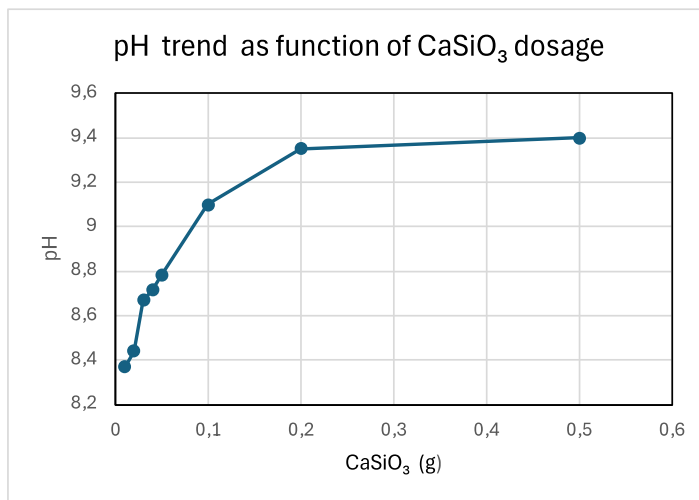


Figure 6. pH trend as a function of calcium silicate dosage

ICP analysis (Figure 7) shows that both calcium and silicon concentrations increase with higher CaSiO₃ loading. Calcium rises from approximately 4.1 to 6.1 mg/dL, while silicon increases from about 0.8 to 4.0 mg/dL. This confirms that the solid dissolves in water, releasing measurable amounts of both ions. The curve flattens at higher additions, indicating that solubility limits are being approached.

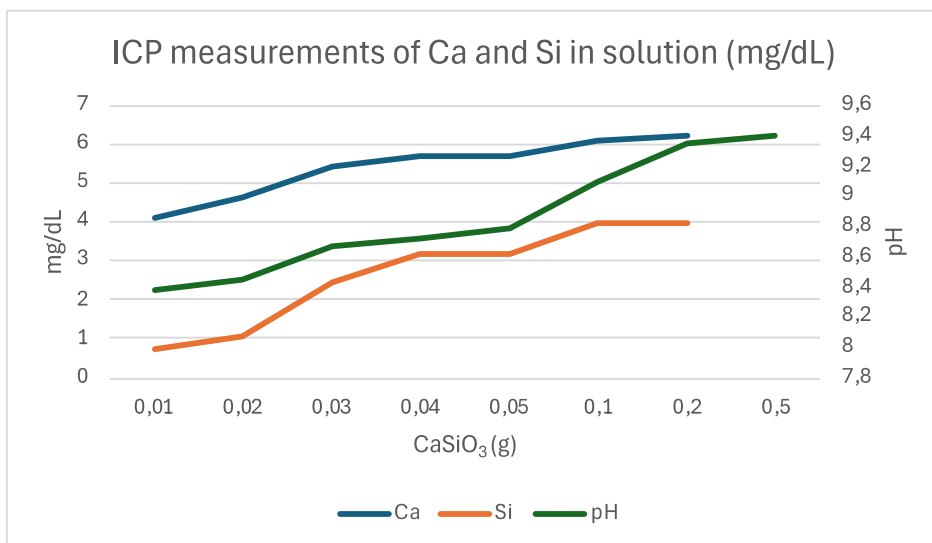


Figure 7. ICP measurements of Ca and Si in solution (mg/dL)

When the ICP data are recalculated into mmol/dL (see figure 8), a clearer view of the dissolution pattern emerges. Calcium increases from roughly 0.001 to 0.00155 mol/dL (equivalent to 0.155 mmol/mL), and silicon follows a similar trend. These values affirm that significant dissolution occurs, though the approaching plateau implies saturation behavior.

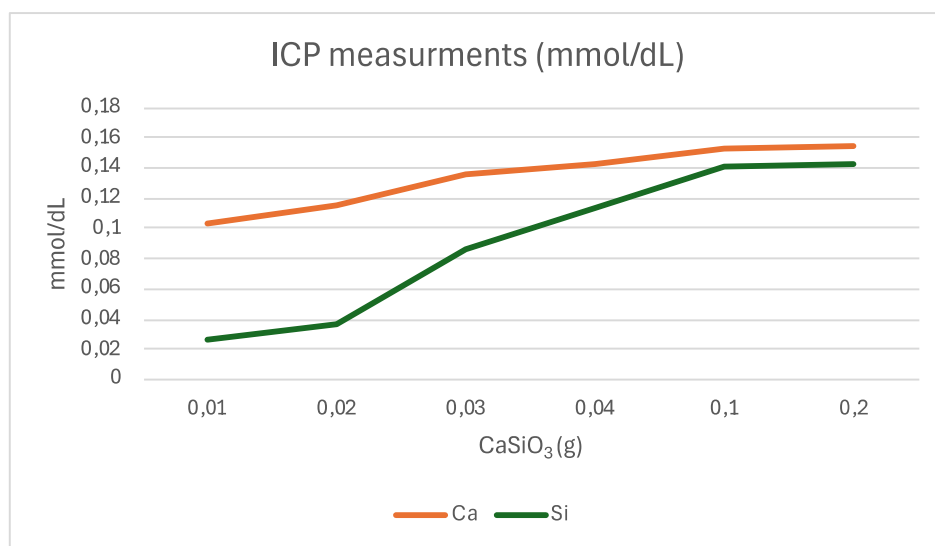


Figure 8. . Converted ICP concentrations (mmol/dL) of Ca and Si

ISE results (see Figure 9) show a rising trend in free calcium ions from 0.005 to just over 0.02 mmol/dL, accompanied by the increasing pH. However, some fluctuation is observed, especially around the mid-range concentrations. This

variability may result from experimental sensitivity, pH effects on ion activity, or partial formation of calcium-containing complexes, reducing the free Ca^{2+} fraction in this section.

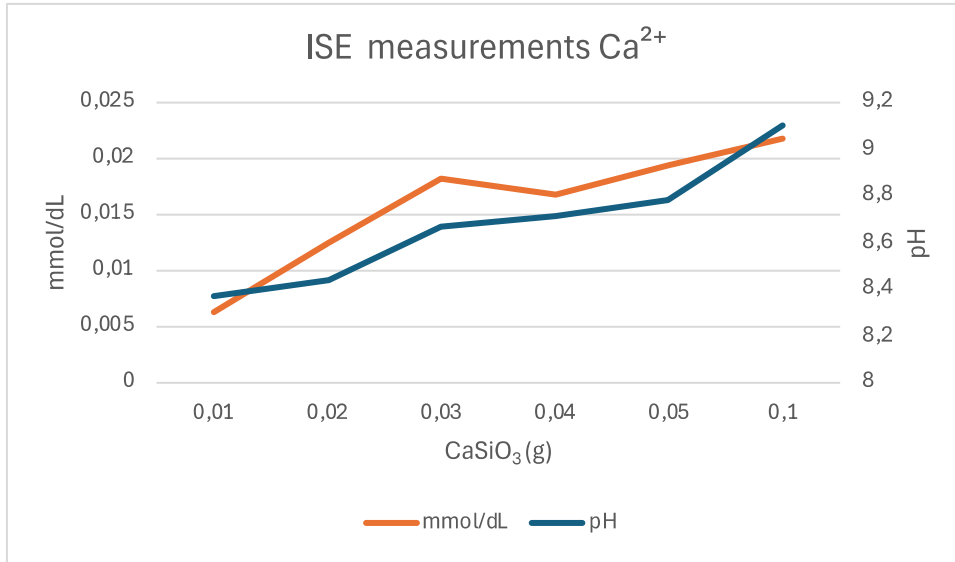


Figure 9. ISE measurements of free Ca^{2+} (mmol/dL) and pH

Figure 10 directly compares total calcium from ICP to free calcium from ISE. It is evident that free Ca^{2+} measured by ISE is consistently lower than the total calcium, especially at higher concentrations. This suggests that not all dissolved calcium remains in ionic form—some is likely bound in silicate species or begins to precipitate at elevated pH values. This divergence emphasizes the importance of distinguishing between total and bioavailable ion concentrations in solubility studies.

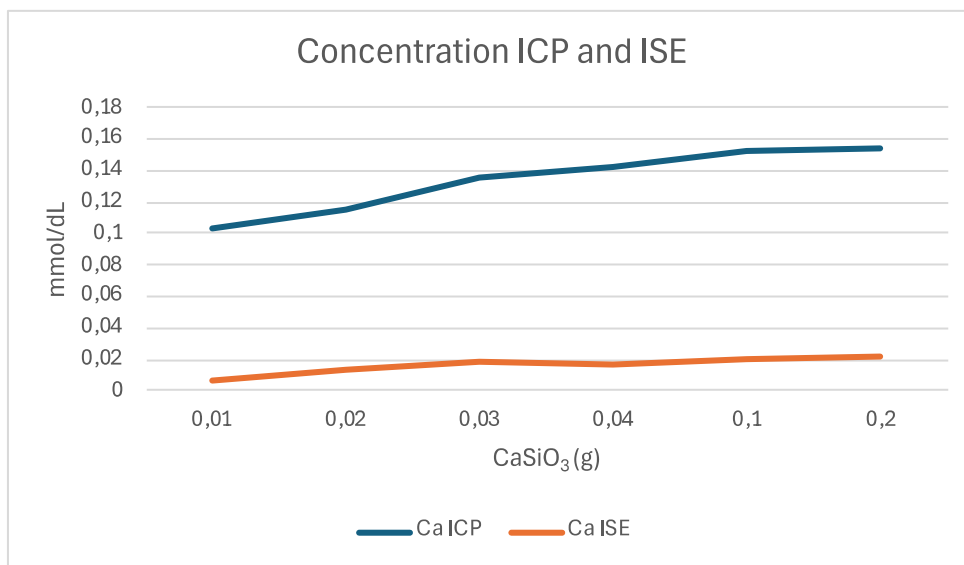


Figure 10. Comparison of total Ca (ICP) vs. free Ca²⁺ (ISE)

4.2 Solubility in co-solvents

In line with the theoretical framework discussed earlier—particularly the effect of pH and complexation on calcium silicate solubility—this section evaluates the influence of citric acid (C₆H₈O₇) as a co-solvent on CaSiO₃ dissolution.

Two citric acid concentrations (0.035% and 0.07%) were tested. Citric acid is known to lower solution pH and act as a chelating agent via its three carboxylic acid groups, forming stable calcium–citrate complexes.

The initial pH values in both citric acid solutions were significantly lower than in water alone, starting around pH 2.5–3.5 depending on acid concentration (Figure 11 & 12). Upon addition of CaSiO₃, the pH gradually increased, consistent with the partial neutralization of the acid and release of OH⁻ ions from hydrolysis reactions.

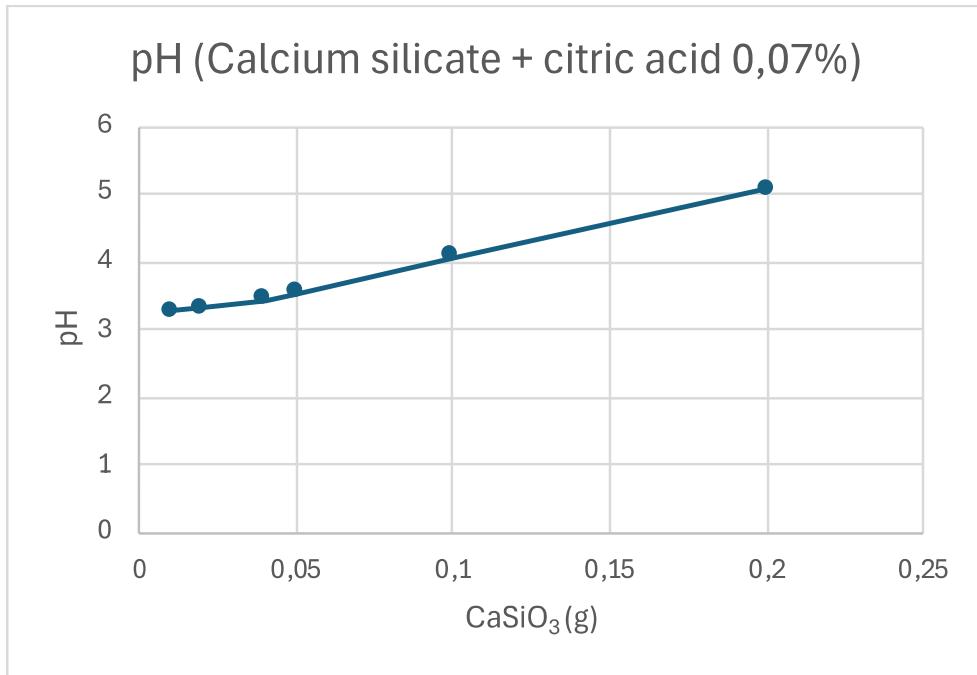


Figure 11. pH trend with citric acid 0,07%

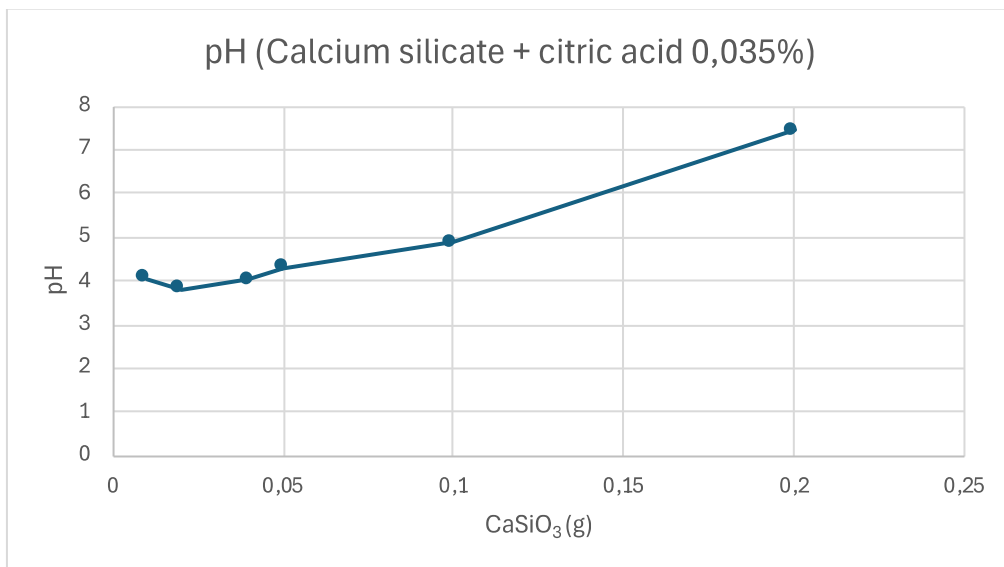


Figure 12. . pH trend with citric acid 0,035%

However, the final pH remained within the buffering range of citric acid ($pK_{a1} \approx 3.1$), indicating that the acidic environment was maintained despite base release from the solid.

ICP measurements confirmed no increased solubility of CaSiO₃ in citric acid compared to pure water (Figures 13 & 14). Calcium concentrations rose with increasing CaSiO₃ addition, reaching approximately 5 mg/dL in 0.07% citric acid and 2,6 mg/dL in 0,035% citric acid. This trend do not support the hypothesis that

low pH enhances calcium ion release by shifting the dissolution equilibrium (Le Chatelier's principle).

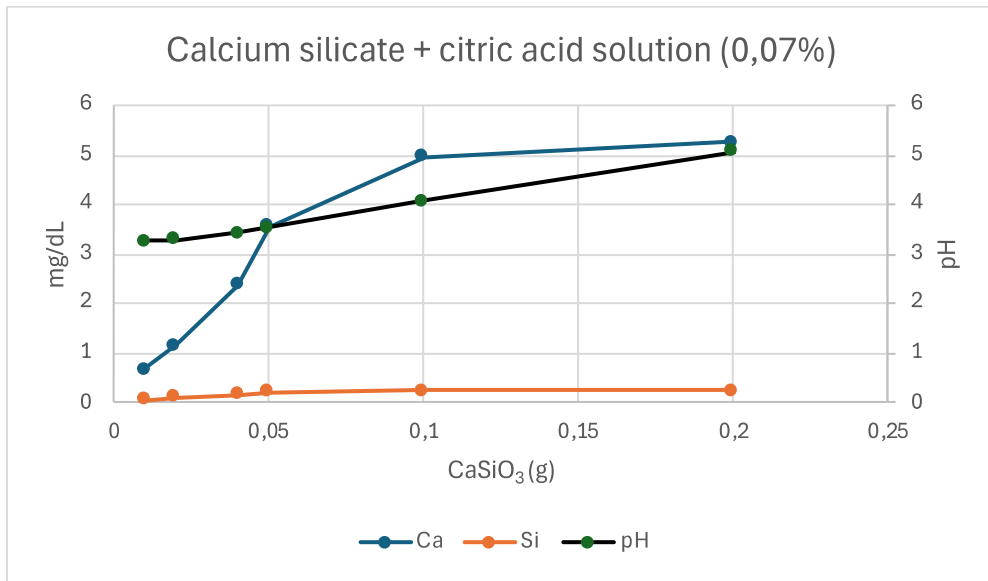


Figure 13. . ICP Analysis Ca and Si, citric acid 0,07%

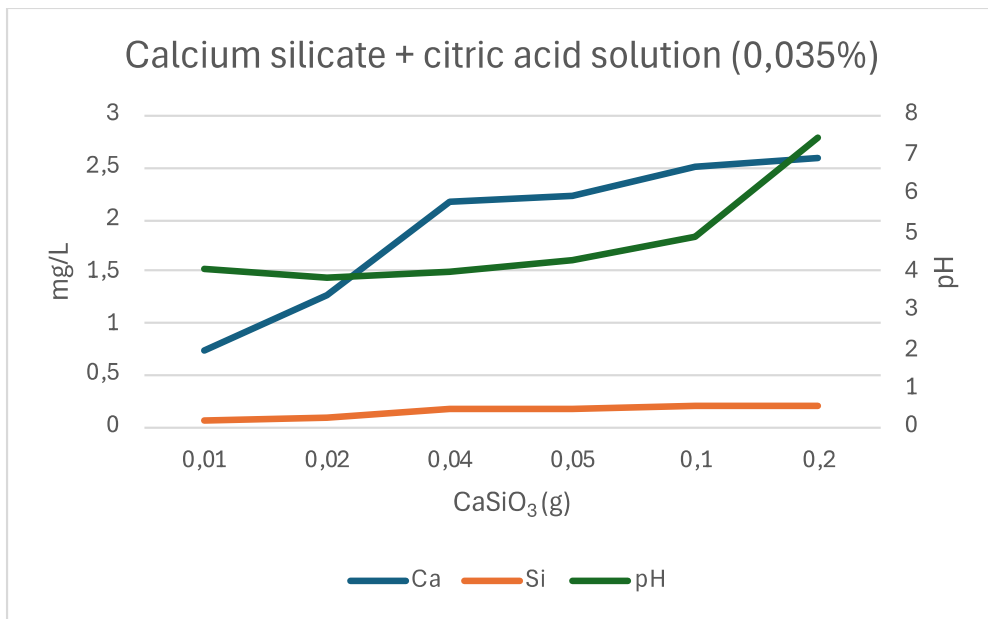


Figure 14. . ICP Analysis Ca and Si, citric acid 0,035%

When converted into molar units (Figure 15 & 16), calcium concentrations reached ~0.065 mmol/dL (0.035% acid) and ~0.14 mmol/dL (0.07% acid). Which indicates a much lower concentration in the acid concentration 0,035% compared to in only water and approximately the same at the acid concentration 0,07% with

higher amount of calcium silicate. When looking at silicon concentration it is lower then the results from the experiments with only water.

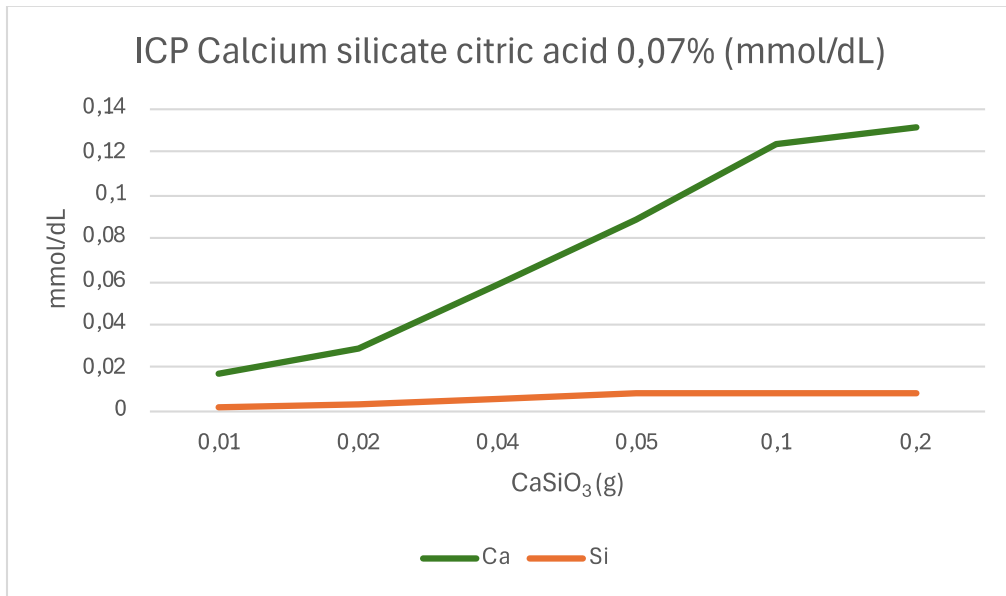


Figure 15. ICP results converted to mmol/dL, citric acid 0,07%

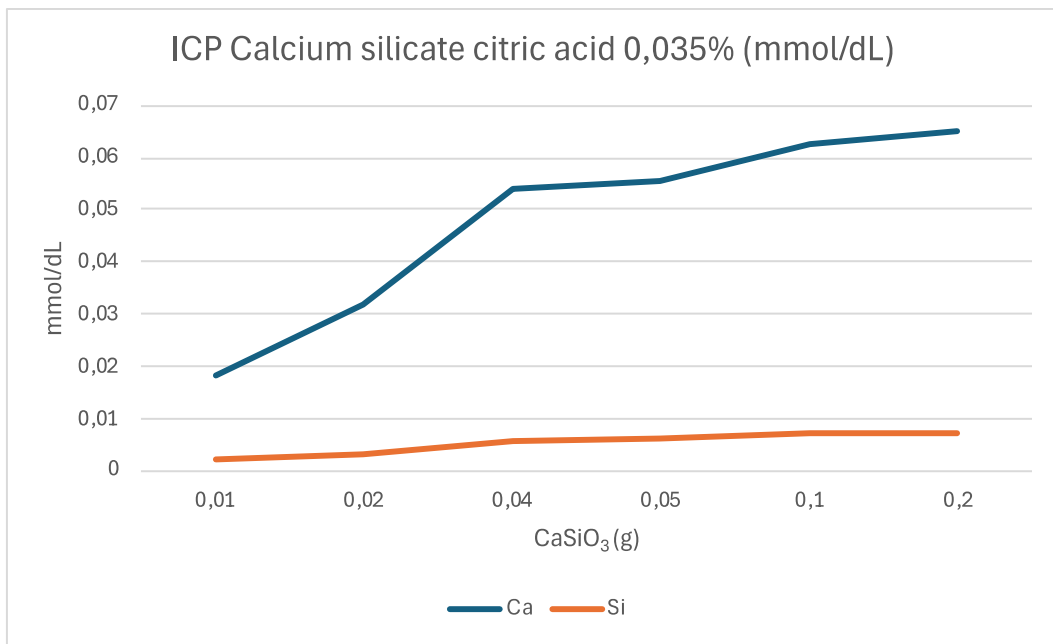


Figure 16. ICP results converted to mmol/dL, citric acid 0,035%

Interestingly, the ISE data revealed that free Ca²⁺ ion activity increased in both acidic systems, with concentrations peaking around 0.16 mmol/dL in 0.07% citric acid (see Figure 17) and 0.13 mmol/dL in 0.035% citric acid (see Figure 18). The rise in free calcium despite complexation indicates that calcium–citrate complexes

in this system are either weakly bound or partially dissociated, maintaining a dynamic equilibrium that favors free ion presence—reinforcing the theory.

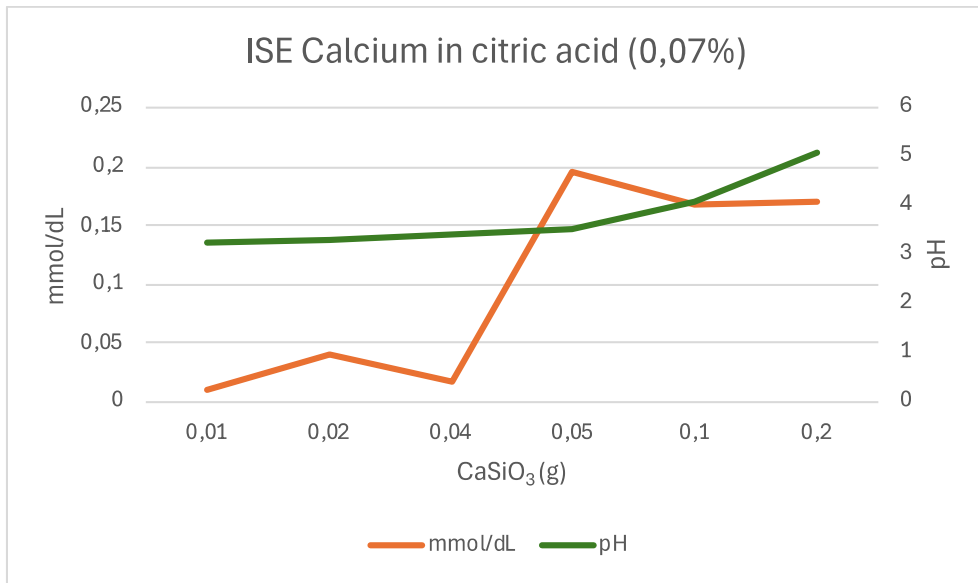


Figure 17. ISE measurements of free Ca^{2+} , solution with citric acid 0,07%

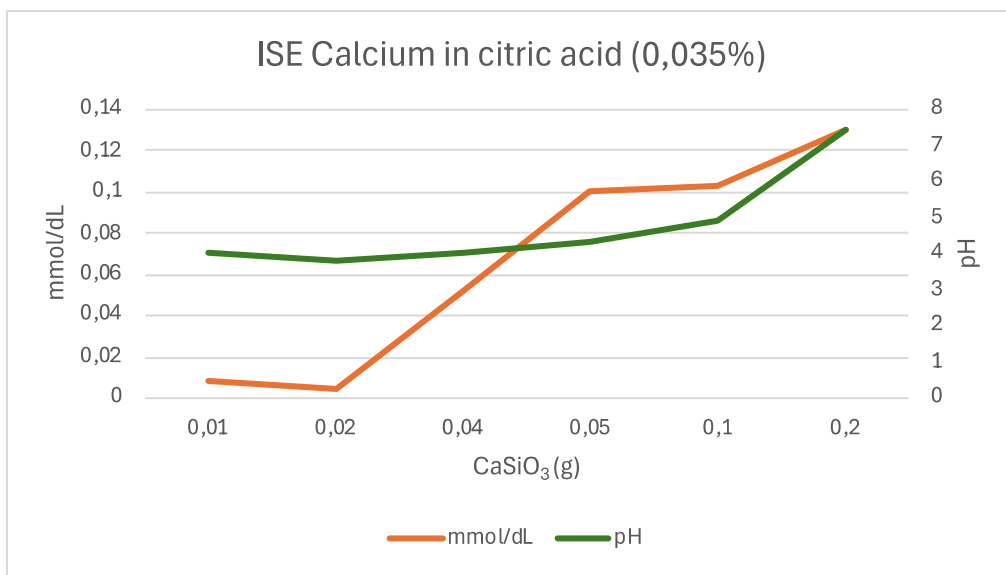


Figure 18. ISE measurements of free Ca^{2+} , solution with citric acid 0,035%

A direct comparison between ICP (total Ca) and ISE (free Ca^{2+}) shows that while citric acid does not enhance the solubility when looking at ICP, the opposite is shown with ISE.

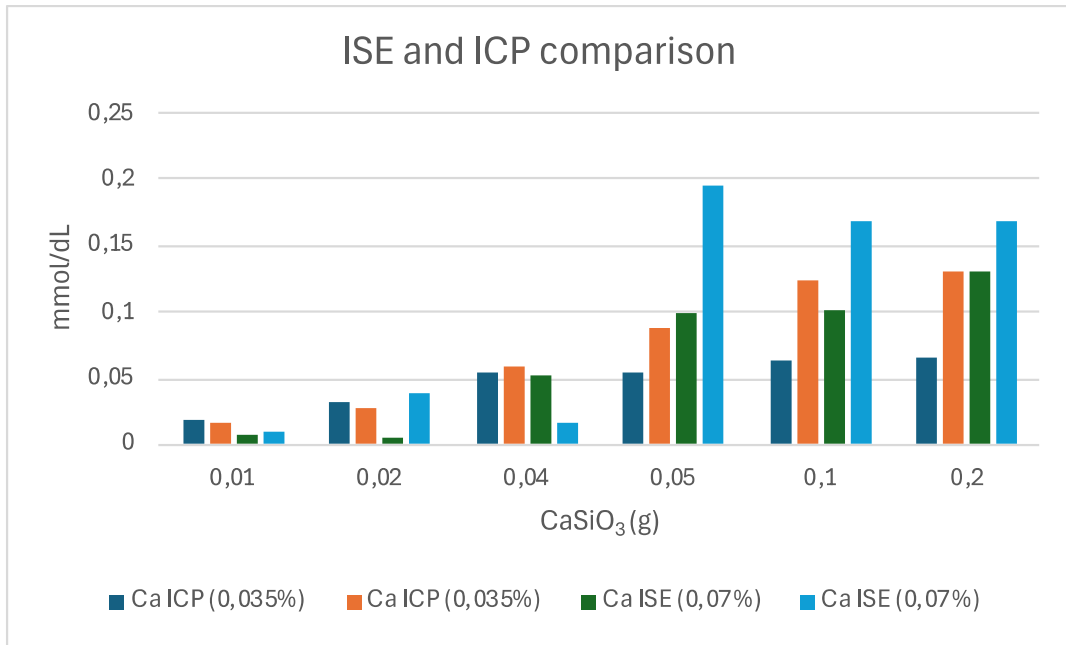


Figure 19 ICP and ISE comparison Ca^{2+} concentration

4.3 Solubility in NPK solution

In this preliminary experiment, calcium silicate (CaSiO_3) was added to an aqueous NPK fertilizer solution in increasing concentrations (0.01–0.5 g/100 mL), and the resulting pH and calcium ion activity were measured using a pH meter and ion-selective electrode (ISE).

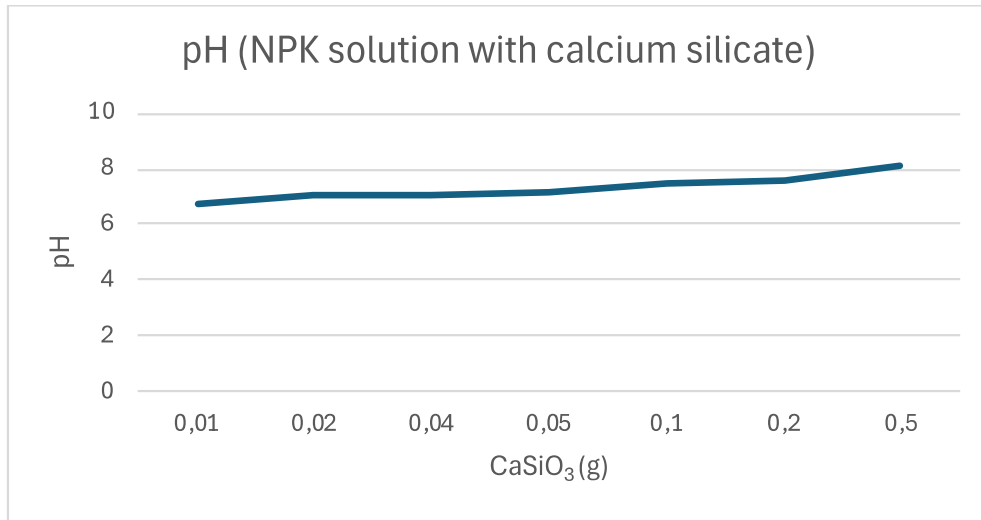


Figure 20. pH in NPK Solution with Calcium Silicate

The pH trend (Figure 19) indicates a gradual increase with higher amounts of CaSiO₃, rising from ~6.8 to 8.4. This is consistent with the expected hydrolysis of calcium silicate, which releases hydroxide ions and shifts the solution towards alkalinity, although the NPK solution appears to buffer the pH to some extent.

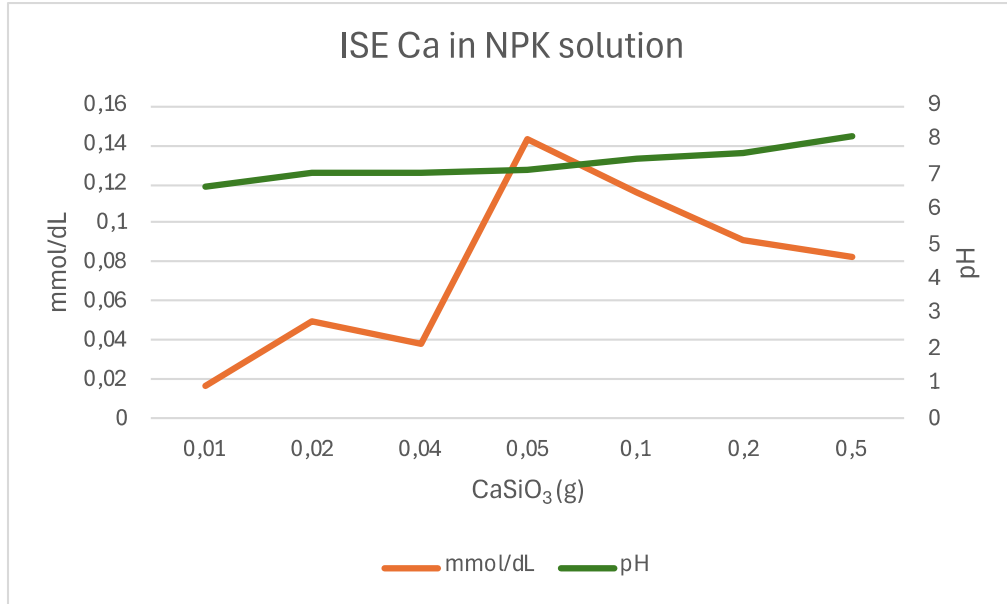


Figure 21. Free Ca²⁺ Activity Measured by ISE

ISE data (Figure 20) showed a peak in free calcium ion activity around 0.05–0.1 g CaSiO₃ addition (~0.15 mmol/dL), followed by a decline at higher concentrations. This suggests that at higher CaSiO₃ levels, either precipitation (e.g. calcium phosphate formation) or complexation may be reducing the availability of free

Ca²⁺ ions in solution. The total concentration of Ca²⁺ ions in the solution is higher than in the experiments with only water.

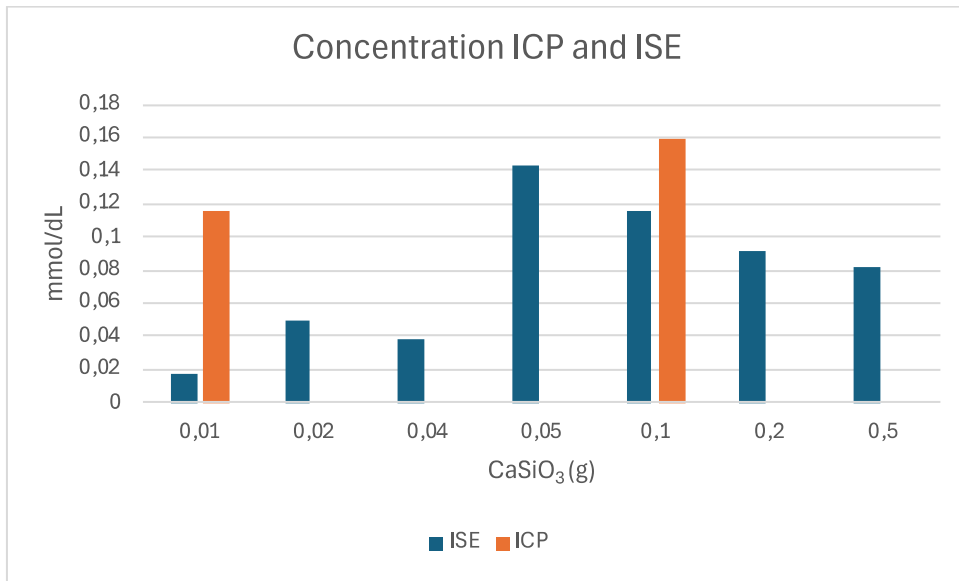


Figure 22. Comparison of ISE and ICP

Currently, only ISE measurements are available. The concentration of free Ca²⁺ alone does not provide the full picture of calcium availability (see figure 21). In future work, ICP-OES analysis should be performed on these samples to quantify the total dissolved calcium and silicon, enabling a complete comparison with free ion concentrations.

4.3.1 TGA

The core aim was to explore how calcium silicate dissolves or reacts in the aqueous NPK environment. Calcium silicate is only sparingly soluble in pure water, but in nutrient-rich acidic or ionic solutions, such as those containing phosphate, and potassium, partial dissolution or surface reaction may occur. These conditions promote the release of Ca²⁺ and silicate (SiO₄⁴⁻/H₄SiO₄) ions, which can further interact with phosphate (PO₄³⁻) to form amorphous calcium phosphate or phosphosilicate phases.

For the sample with 0.001 g CaSiO₃, the TGA curve (see figure 22) showed a total weight loss of approximately 68%, divided across five steps.

- 25–150 °C: Evaporation of residual water and loosely bound moisture.
- 150–250 °C : Decomposition of salts, nitrates, and water-soluble phosphate species.

- 250–350 °C : Further breakdown of polyphosphates and partially decomposed organic NPK components.
- 350–500 °C : Thermal degradation of potassium-containing compounds, and possible reactions between NPK residues and the small amount of silicate.
- >600 °C : Minor decomposition of residual organics or unstable intermediate phases.

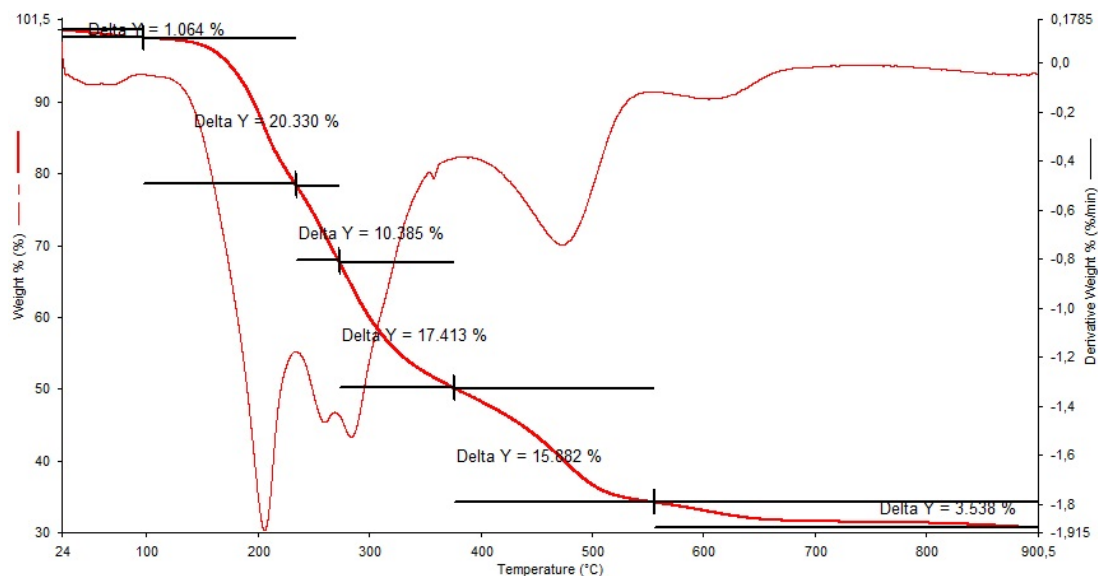


Figure 23. The TGA curve of sample NPK + 0.001 g CaSiO₃

The 0.01 g CaSiO₃ sample displayed a slightly different behavior, with a more pronounced early-stage loss (1.6%) and larger mid-range degradation steps (17.9%, 28.0%, 15.7%), consistent with the original decomposition profile observed earlier:

- <150°C: Moisture evaporation.
- 150–250°C: Ammonium and nitrate breakdown.
- 250–400°C: Phosphate and organic compound decomposition.
- 400–550°C: Likely interaction between calcium silicate and decomposed NPK species (formation of amorphous phosphosilicates or calcium phosphate compounds).
- >600 °C: Residual loss from carbonate-like impurities or rearrangement

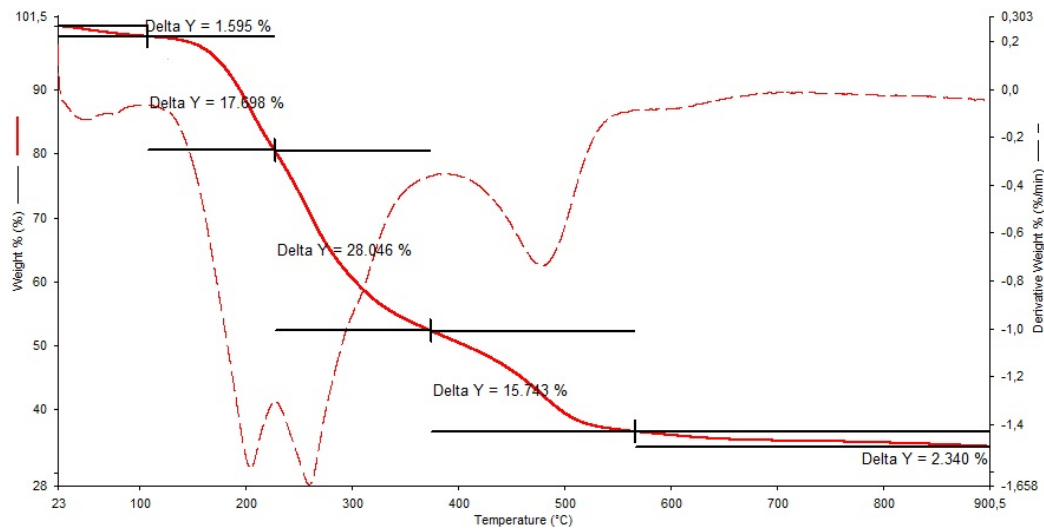


Figure 24. TGA curve of sample NPK + 0.01 g CaSiO_3

The TGA profile of the sample containing NPK and 1 g of calcium silicate displays a five-step decomposition pattern, as shown in Figure 24. The overall weight loss is relatively low compared to samples with lower CaSiO_3 content, indicating that most of the added calcium silicate remains thermally stable throughout heating.

- 25–150°C: Corresponds to evaporation of free and bound moisture, including residual water in the matrix and potentially surface-adsorbed water on CaSiO_3 particles.
- 150–200°C: Likely caused by initial decomposition of ammonium salts or low-molecular NPK components.
- 200–300°C: Represents continued decomposition of nitrate- or phosphate-based fertilizer components. Minimal loss indicates limited NPK interaction with CaSiO_3 .
- 300–500°C: This broader mass loss is primarily attributed to decomposition of more stable organophosphates, sulfur compounds, or minor NPK–silicate interactions.
- 500–800°C: Final mass loss, likely from carbonates or trapped organics, or slight rearrangement of silicate structures.

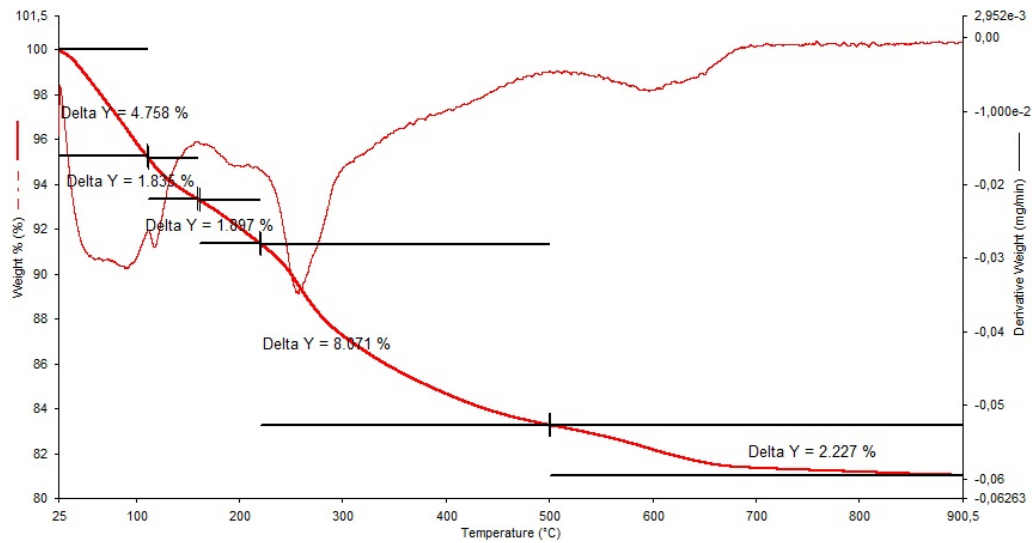


Figure 25. TGA curve on sample containing NPK + 1 g CaSiO_3

4.3.2 SEM-EDS

To further investigate the chemical behavior of calcium silicate in the NPK environment, SEM-EDS analysis was performed on the same thermally treated samples.

In the 0.001 g CaSiO_3 sample, EDS revealed low amounts of Si (2.5%) and Ca (1.1%), while K (15.4%) and P (4.1%) dominated the profile. This indicates that most of the calcium silicate dissolved, supporting the release of Ca^{2+} and silicate ions into the solution. The morphology appeared fine-grained and non-crystalline.

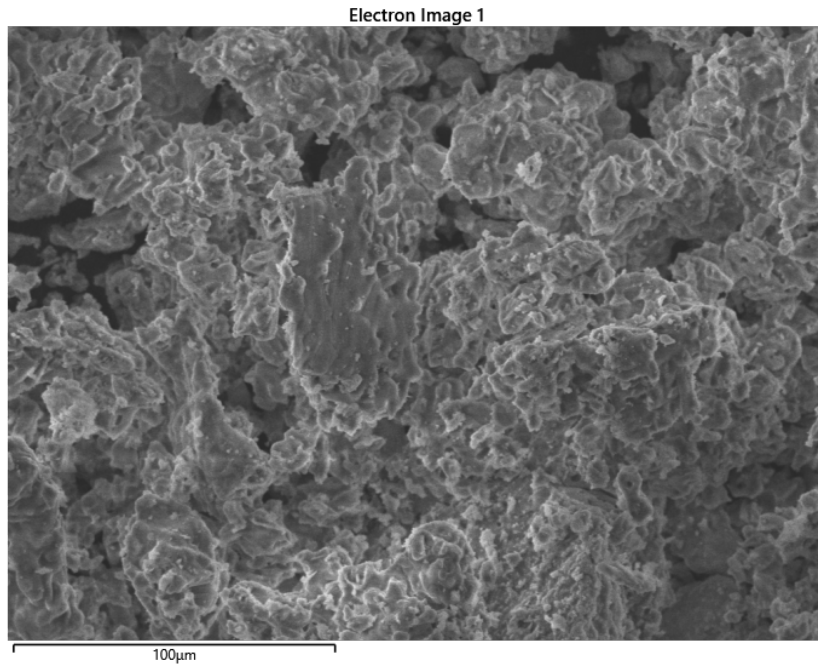


Figure 26. SEM image of 0.001 g CaSiO_3 sample

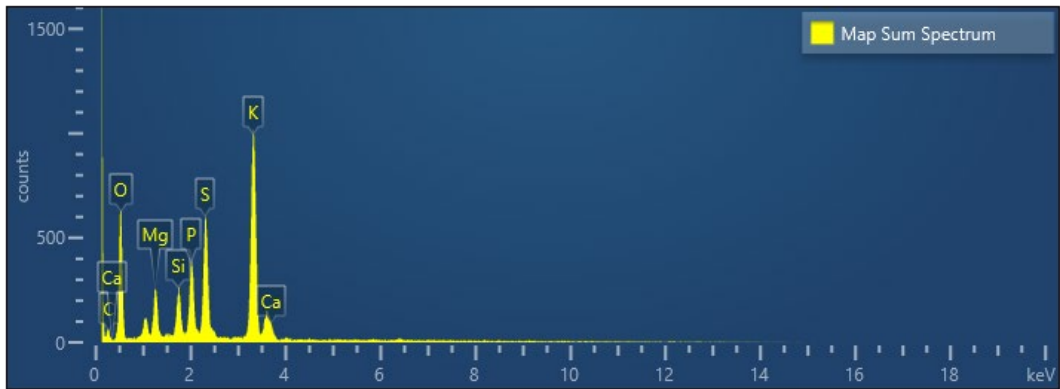


Figure 27. Sum spectrum map of 0.001 g CaSiO_3 sample

Table 2. Map Sum Spectrum table of content of 0.001 g CaSiO₃ sample

Map Sum Spectrum				
Element	Line Type	Weight %	Weight % Sigma	Atomic %
C	K series	2.37	4.04	4.35
O	K series	43.68	1.93	60.32
K	K series	27.19	1.21	15.36
Si	K series	3.18	0.19	2.50
P	K series	5.75	0.31	4.10
S	K series	10.22	0.49	7.04
Mg	K series	3.77	0.23	3.42
Ca	K series	1.95	0.21	1.08
Na	K series	1.90	0.19	1.82
Total		100.00		100.00

For the 0.01 g CaSiO₃ sample, EDS spectra indicated Si (9.5%), Ca (2.2%), K (8.3%), and P (2.8%), showing greater incorporation of NPK-derived elements and partial dissolution of calcium silicate (see figures 27, 28 and table 3).

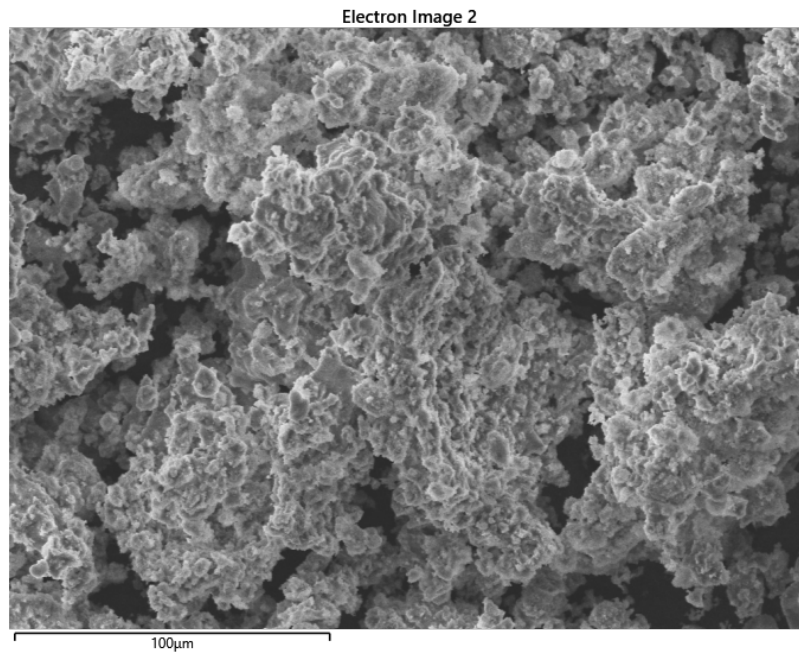


Figure 28. SEM image of 0.01 g CaSiO_3 sample

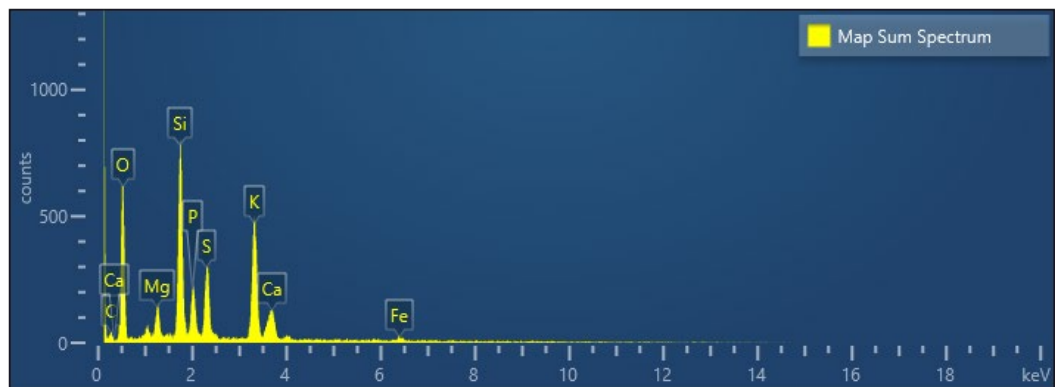


Figure 29. Sum spectrum map of 0.01 g CaSiO_3 sample

Table 3. Map Sum Spectrum table of content of 0.01 g CaSiO_3 sample

Map Sum Spectrum				
Element	Line Type	Weight %	Weight % Sigma	Atomic %
C	K series	5.87	4.51	10.15
O	K series	45.74	2.30	59.33
Si	K series	12.82	0.68	9.48
K	K series	15.55	0.82	8.25
S	K series	6.59	0.39	4.26
Mg	K series	2.43	0.19	2.07
P	K series	4.17	0.29	2.79

Ca	K series	4.25	0.32	2.20
Fe	K series	1.62	0.36	0.60
Na	K series	0.97	0.16	0.87
Total		100.00		100.00

In the 1 g CaSiO_3 sample, EDS showed high atomic percentages of Si (29.9%) and Ca (4.3%), with low levels of K (0.7%) and P (0.5%), indicating that most of the calcium silicate remained undissolved and was not released as free ions.

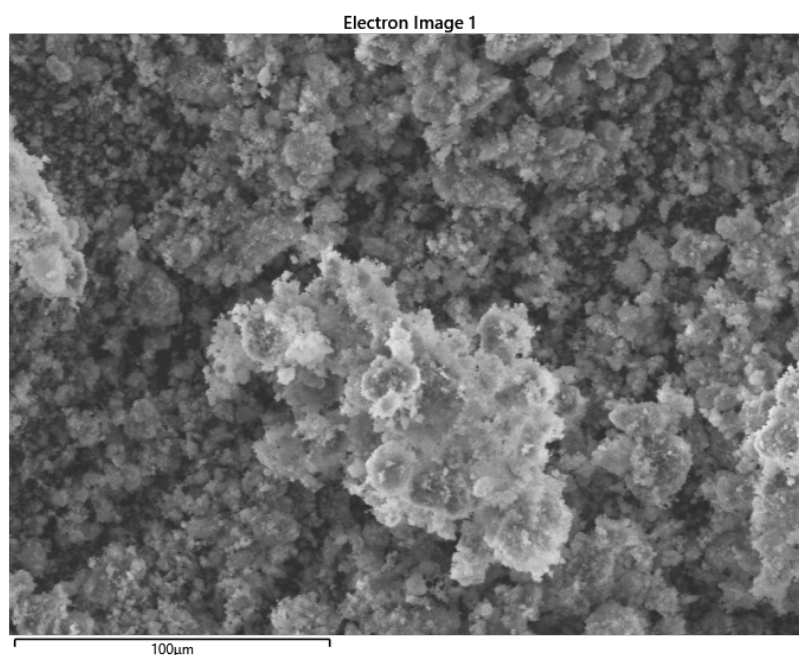


Figure 30. SEM image of 1 g CaSiO_3 sample



Figure 31. Map Sum Spectrum of 1 g CaSiO_3 sample

Table 4. Map Sum Spectrum table of content of 1 g CaSiO₃ sample

Map Sum Spectrum				
Element	Line Type	Weight %	Weight % Sigma	Atomic %
C	K series	0.30	5.34	0.52
O	K series	49.02	2.68	63.93
Si	K series	40.22	2.20	29.88
Ca	K series	8.19	0.50	4.26
K	K series	1.24	0.15	0.66
P	K series	0.71	0.13	0.48
Mg	K series	0.33	0.09	0.28
Total		100.00		100.00

4.3.3 XRD

XRD was used to assess the crystallinity of the ash and detect any remaining calcium silicate or formation of crystalline calcium phosphate phases.

In the 0.001 g CaSiO₃ sample, the XRD pattern lacked defined peaks, consistent with an amorphous structure. The absence of crystalline calcium phosphate confirms that if calcium phosphate was formed, it likely remained amorphous, which is typical for precipitation from solution under mild conditions.

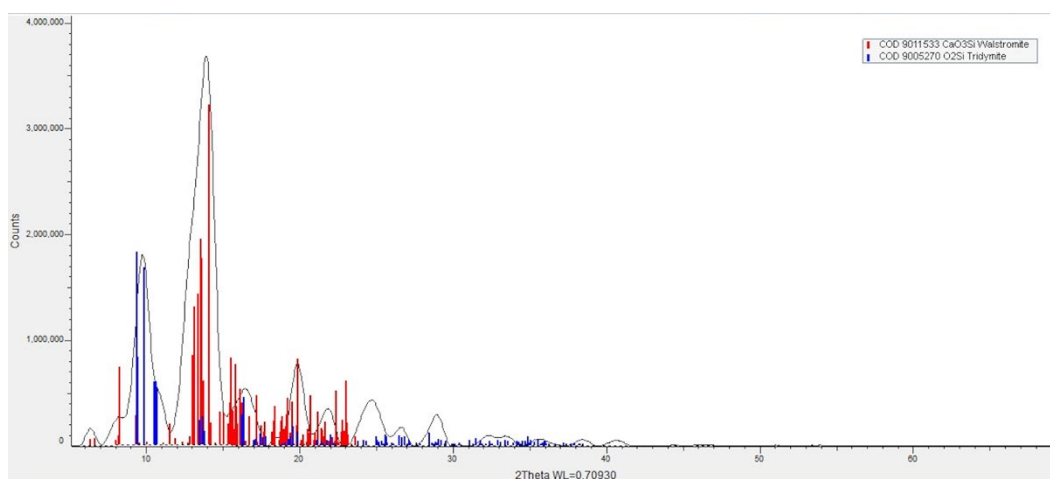


Figure 32. XRD pattern of 0,001 g CaSiO₃ sample

For the 0.01 g CaSiO₃ sample, wollastonite and cristobalite peaks were present but less intense and broader, indicating some level of reaction or partial dissolution. Still, no clear evidence of crystalline calcium phosphate phases such as hydroxyapatite or tricalcium phosphate was found.

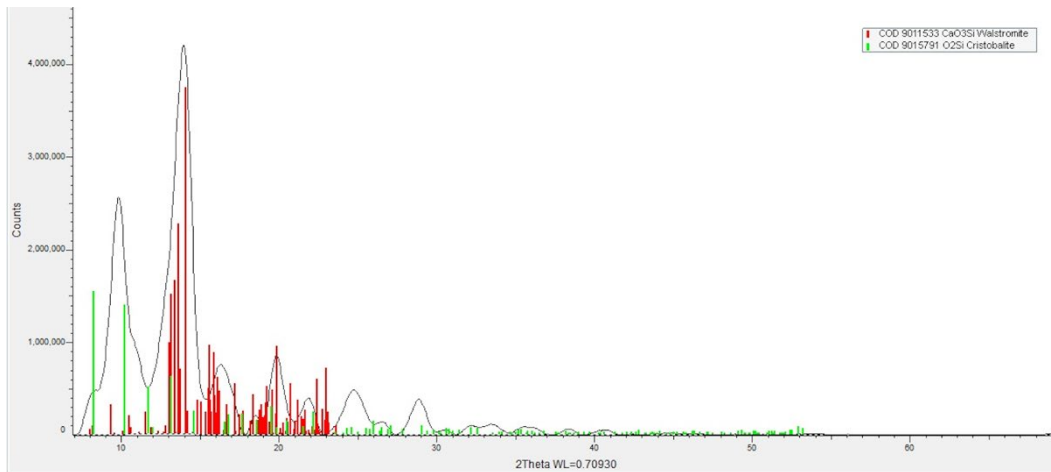


Figure 33. XRD pattern of 0,01g CaSiO_3 sample

In the 1 g CaSiO_3 sample, sharp peaks corresponding to wollastonite were clearly visible, confirming the presence of undissolved calcium silicate. No crystalline phosphate phases were observed, suggesting either complete retention of phosphate in amorphous form or its absence from solid residues.

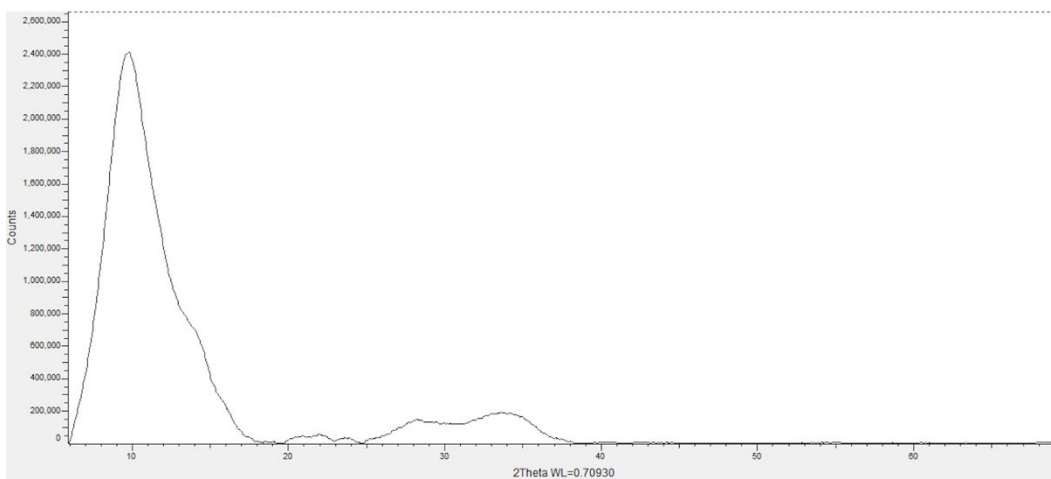


Figure 34. XRD pattern of 1 g CaSiO_3 sample

4.4 Solubility in NPK solutions containing citric acid

To simulate more realistic agricultural conditions, calcium silicate (CaSiO_3) was tested in combination with a commercial NPK (nitrogen–phosphorus–potassium) fertilizer solution and citric acid at two concentrations: 0.035% and 0.07%.

The aim was to investigate how citric acid affects calcium ion availability and pH in phosphate-rich systems, where calcium precipitation would normally reduce solubility.

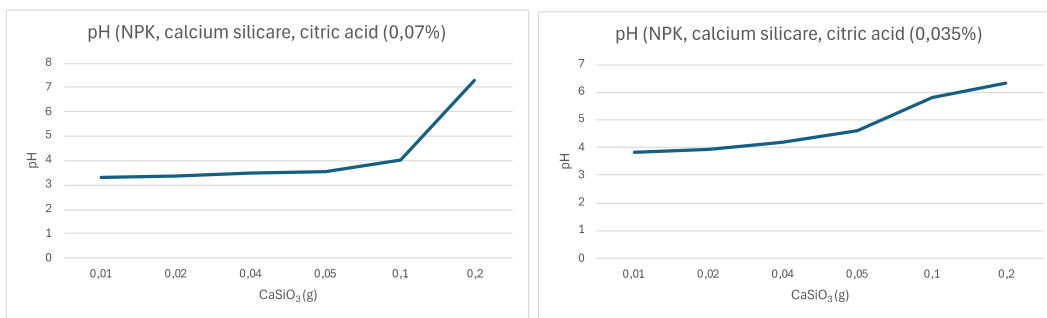


Figure 35 and 36. pH development in NPK + citric acid + CaSiO₃ systems

As shown in Figure 34 and 35, the initial pH of the NPK and citric acid mixture was acidic (~3.5–4), but increased with added CaSiO₃. At the highest dosage (0.2 g/100 mL), the pH reached 6.2–7.2. This rise is attributed to hydroxide ion release from calcium silicate, which partially neutralized the acidic environment.

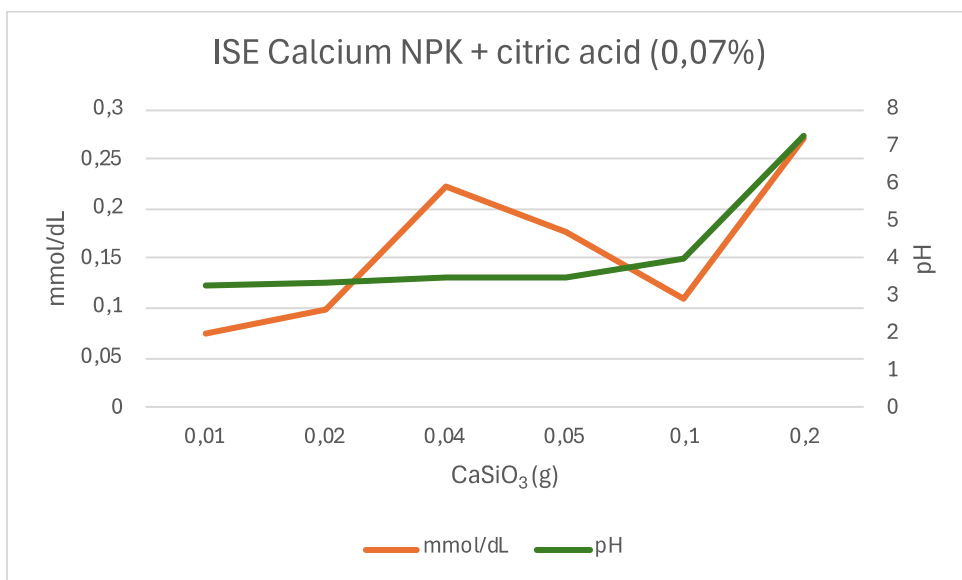


Figure 37. ISE measurements of free Ca²⁺ in 0.07% citric acid

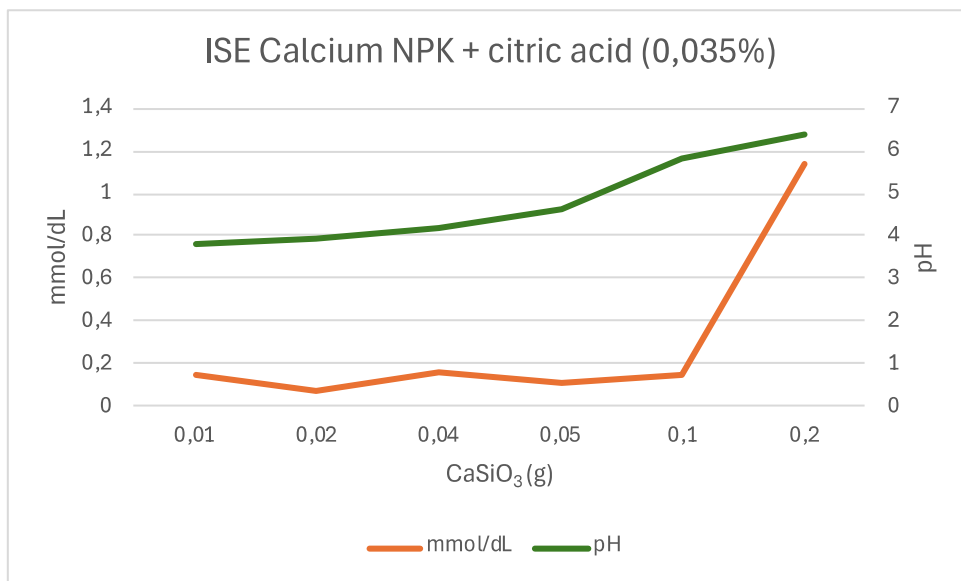


Figure 38. ISE measurements of free Ca²⁺ in 0.07% citric acid

Figures 36 and 37 display the free calcium ion concentrations measured by ISE in the two citric acid treatments. At 0.035%, free Ca²⁺ levels increased sharply with added CaSiO₃, reaching a peak of approximately 1.1 mmol/dL. In contrast, the 0.07% solution showed a smaller increase, with levels stabilizing around 0.07–0.3 mmol/dL. These differences suggest that while both acid levels improve calcium solubility, the lower concentration allows for greater availability of free Ca²⁺.

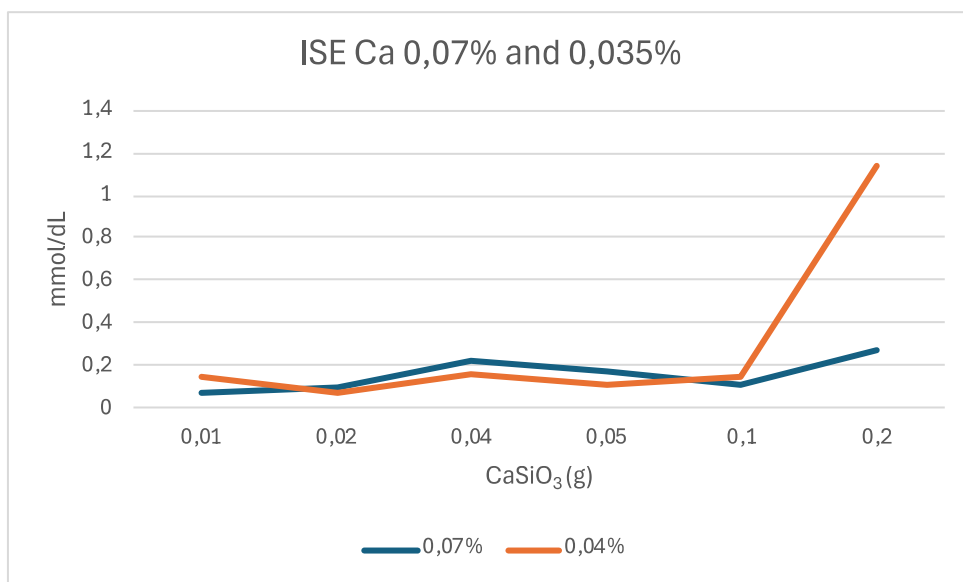


Figure 39. Comparison of ISE values between 0.035% and 0.07% citric acid

Figure 38 directly compares the two solutions and highlights that 0.035% citric

acid consistently yields higher free Ca^{2+} concentrations at every CaSiO_3 level. This outcome may reflect an optimal balance: enough acid to increase solubility, but not so much that it overly complexes the calcium ions.

Although citric acid is theoretically expected to reduce free Ca^{2+} concentrations through chelation, the opposite trend was observed.

4.4.1 TGA

To further investigate the solubility behavior of calcium silicate in NPK systems, a new sample was prepared by dissolving NPK and CaSiO_3 in water, with the addition of citric acid as a complexing agent. After 48 hours of drying, the sample was subjected to thermogravimetric analysis.

The TGA curve of the citric-acid-modified sample (see Figure 39) displayed multiple weight loss steps, similar in pattern to the non-acidified systems but with distinct differences in intensity and temperature range.

- Below 150 °C: A slightly higher mass loss was observed compared to earlier samples, attributed to retained moisture.
- 150–300 °C: A major weight loss occurred, indicating decomposition of phosphates, and Ca–citrate complexes. The presence of citric acid likely facilitated more extensive dissolution of CaSiO_3 , followed by thermal decomposition of the resulting calcium citrate.
- 300–500 °C: Continued mass loss suggested degradation of organic residues and phosphate components.
- >500 °C: A stable plateau indicated that most reactive species had decomposed, and a mineral residue (possibly silicate or phosphate salts) remained.

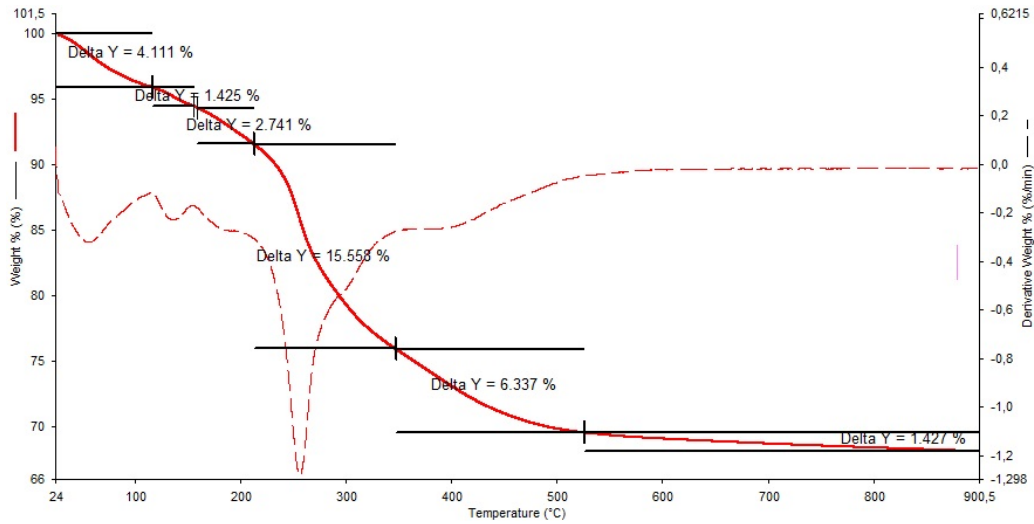


Figure 40. *CaSiO₃_NPK_Citric acid_*

4.4.2 SEM-EDS

SEM imaging (Figure 40) revealed a porous, amorphous structure without visible crystalline phases. The surface was fine-textured and lacked the dense particles seen in high- CaSiO_3 systems, suggesting dissolution of the solid material.

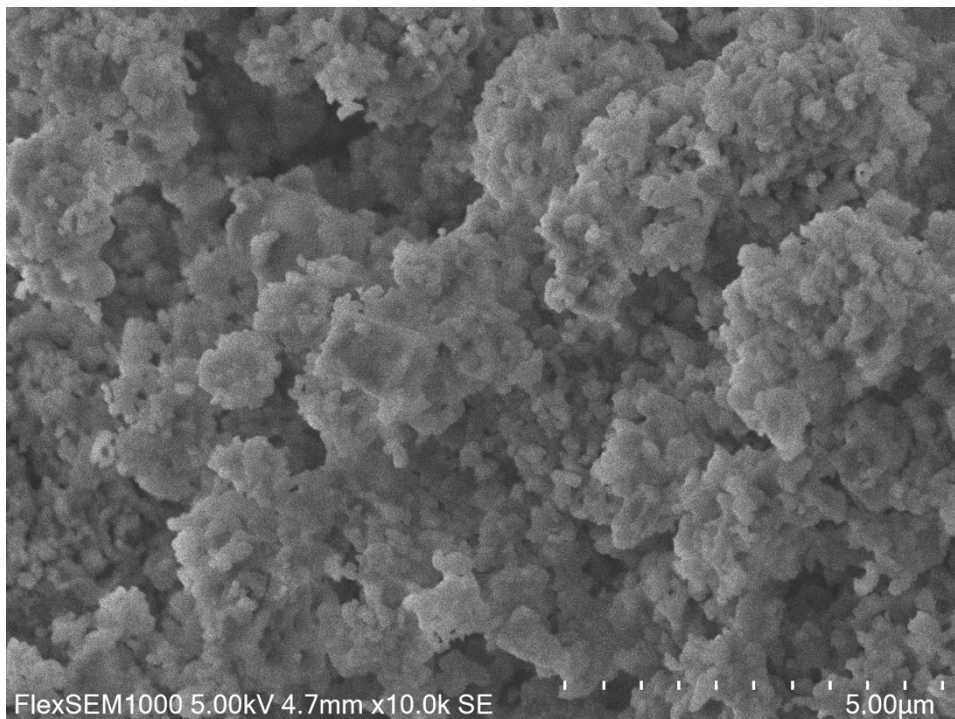


Figure 41. *SEM image of NPK+Citric acid+CaSiO₃*

EDS analysis (Figure 41 and 42) of the residue showed high proportions of oxygen (~63%) and silicon (~23%), with calcium present at ~2% and phosphorus at 1%. Potassium were also detected, consistent with NPK composition. The co-occurrence of Ca and P with no crystalline phases suggests the presence of amorphous calcium phosphate.

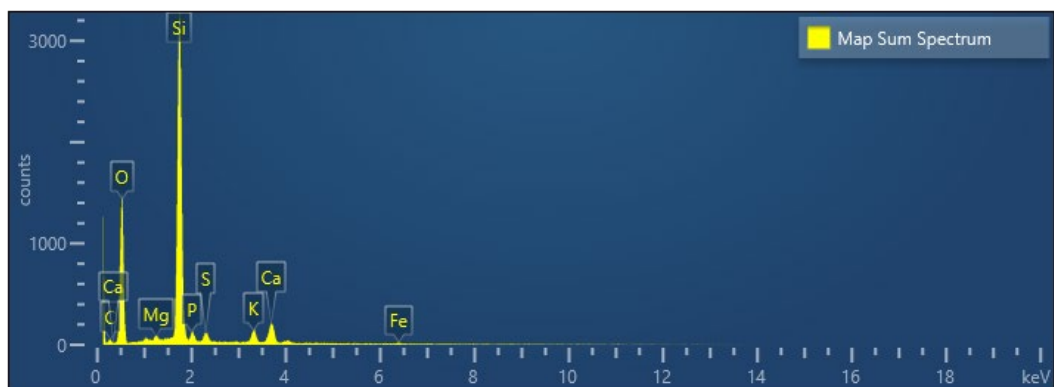


Figure 42. EDS analysis of elemental composition

Table 5. EDS composition table

Map Sum Spectrum				
Element	Line Type	Weight %	Weight % Sigma	Atomic %
C	K series	3.89	4.52	6.44
O	K series	51.04	2.45	63.49
Si	K series	33.08	1.60	23.44
K	K series	2.58	0.18	1.31
Ca	K series	4.70	0.28	2.33
P	K series	1.55	0.15	1.00
Mg	K series	0.54	0.09	0.44
S	K series	1.44	0.13	0.90
Na	K series	0.46	0.11	0.39
Fe	K series	0.71	0.23	0.25
Total		100.00		100.00

4.4.3 XRD

The XRD pattern (Figure 42) confirmed the absence of sharp crystalline peaks.

The XRD pattern (Figure 42) shows peaks, indicating the presence of pseudowollastonite (CaSiO_3) and cristobalite (SiO_2). This is based on reference patterns from the COD database. These results suggest that calcium silicate, when added to the NPK + citric acid system, does not dissolve completely but instead contributes to the formation of crystalline silicate and silica phases. This indicates limited solubility in the media.

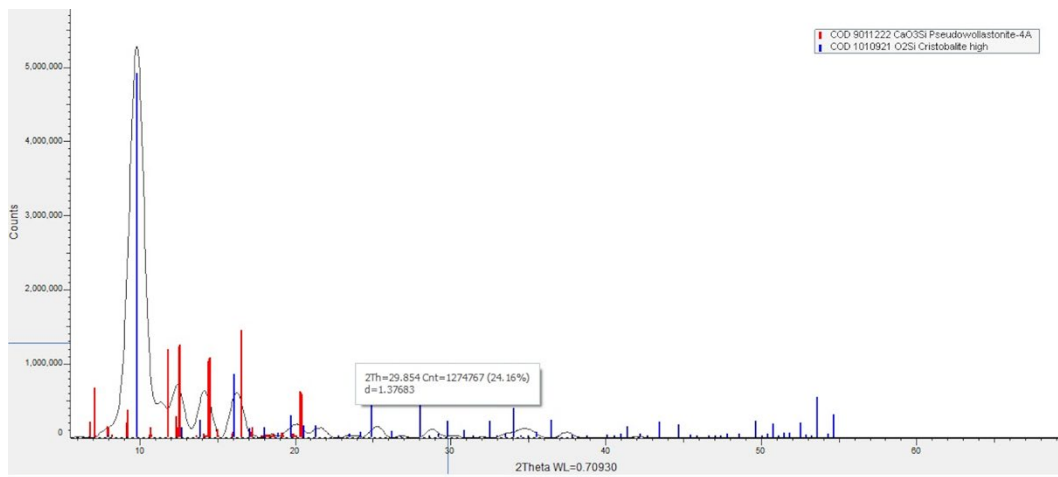


Figure 43. XRD diffractogram of NPK+Citric acid+ CaSiO_3

5. Conclusions

This study confirms that calcium silicate (CaSiO_3) shows limited solubility in pure water, primarily due to its high lattice enthalpy and the weak hydration of its anionic components. Although some dissolution occurs the free Ca^{2+} concentration quickly plateaus, suggesting limited bioavailability and potential for precipitation or complexation at higher concentrations.

In NPK solutions, the solubility of CaSiO_3 is slightly improved, likely due to ionic interactions and buffering effects. However, free Ca^{2+} activity (measured by ISE) peaks and then decreases with increasing solid addition. This pattern suggests secondary precipitation reactions, particularly with phosphate ions, leading to the formation of calcium phosphate species—an effect confirmed indirectly through TGA and supported by reduced Ca^{2+} availability.

The addition of citric acid has impact on solubility behavior. Although ICP results indicate no substantial increase in total dissolved calcium, ISE measurements show higher levels of free Ca^{2+} in the citric acid systems, especially at the 0.035% concentration. This suggests that citric acid promotes partial dissolution of calcium silicate, possibly by preventing phosphate precipitation through calcium-citrate complexation.

In NPK + citric acid systems, a clear enhancement in calcium ion availability was observed. Free Ca^{2+} levels increased, pH rose moderately, and XRD revealed the presence of crystalline pseudowollastonite and cristobalite, indicating incomplete dissolution but also a shift in solid-phase composition. SEM-EDS analysis supported the formation of mixed amorphous residues, consistent with partial reaction of CaSiO_3 in the acidic, phosphate-rich environment.

In conclusion, calcium silicate is poorly soluble in water, moderately reactive in NPK, and shows the most promising behavior in citric acid-containing nutrient solutions in some cases. The use of citric acid, particularly at moderate concentrations, appears to maybe enhance calcium ion availability. These results can support future development of calcium- and silicon-based supplements in agriculture and other aqueous delivery systems.

Future research should investigate more precisely the concentrations of all the difrent systems. And also more detailed, with lower concentrations and more developed systems and long-term plant uptake under field conditions. Investigation of silicon availibilty in all the solutions should also be investigated in more detail.

References

- Alori, E.T., Glick, B.R. and Babalola, O.O. (2017). Microbial phosphorus solubilization and its potential for use in sustainable agriculture. *Frontiers in Microbiology*. 8, 971. <https://doi.org/10.3389/fmicb.2017.00971>
- Alvarenga, L.M., Xavier, T.P., Barrozo, M.A.S., Bancelos, M.S. & Lira, T.S., 2012. Dynamic analysis of reaction kinetics of carton packaging pyrolysis. In: I.A. Karimi & R. Srinivasan, eds. *Computer Aided Chemical Engineering*. Volume 31. Amsterdam: Elsevier, pp.180–184. doi:10.1016/B978-0-444-59507-2.50028-7.
- Atkins, P.W., 1996. *The elements of physical chemistry*. 2nd ed. Oxford: Oxford University Press.
- Aylward G, Findlay T. *SI chemical data*. Australia: John Wiley; 2008.
- Boss, B.C. & Fredeen, J.K., 2004. General characteristics of ICP-OES. In: *Concepts, instrumentation and techniques in inductively coupled plasma optical emission spectrometry*. 3rd ed. Shelton, Connecticut: PerkinElmer, Inc., Chapter 2.
- Carino, A., Ludwig, C., Cervellino, A., Müller, E. & Testino, A., 2018. Formation and transformation of calcium phosphate phases under biologically relevant conditions: Experiments and modelling. *Acta Biomaterialia*, 74, pp.478–489. doi:10.1016/j.actbio.2018.05.027.
- Drukteinis, S., et al. (2024). The impact of citric acid solution on hydraulic calcium silicate-based sealers and root dentin: a preliminary assessment. *Materials*. 17(6), 1351. <https://doi.org/10.3390/ma17061351>
- Dębicz, R. and Wróblewska, K. (2012). The effect of silicon foliar application on the development of seasonal ornamental plants. Part I: *Sanvitalia speciosa* 'Sunbini', *Verbena* 'Patio Blue' and *Portulaca umbraticola* 'Duna Red'. *Acta Agrobotanica*. 64, 99–106. <https://doi.org/10.5586/aa.2011.051>
- Fiume, M.M., et al. (2014). Safety assessment of citric acid, inorganic citrate salts, and alkyl citrate esters as used in cosmetics. *International Journal of Toxicology*. 33(2_suppl), 16S–46S. <https://doi.org/10.1177/1091581814526891>
- Galster, H., 1991. *pH measurement: Fundamentals, methods, applications, instrumentation*. New York: VCH Publishers.
- Goldberg, I. and Rokem, J.S. (2009). Organic and fatty acid production, microbial. In: *Encyclopedia of Microbiology*. Academic Press. Available from: <https://www.sciencedirect.com/science/article/pii/B9780123739445002907>
- Harris, D.C. & Lucy, C.A., 2020. *Quantitative chemical analysis*. New York, NY: Macmillan Learning.
- Johnson, R., Vishwakarma, K., Hossen, M.S., Kumar, V., Shackira, A.M., Puthur, J.T., Abdi, G., Sarraf, M. and Hasanuzzaman, M. (2022). Potassium in plants: growth regulation, signaling, and environmental stress tolerance. *Plant Physiology and Biochemistry*. 172, 56–69. <https://doi.org/10.1016/j.plaphy.2022.01.001>

- Khan, F., Siddique, A.B., Shabala, S., Zhou, M. and Zhao, C. (2023). Phosphorus plays key roles in regulating plants' physiological responses to abiotic stresses. *Plants (Basel)*. 12(15), 2861. <https://doi.org/10.3390/plants12152861>
- Lim, M., et al. (2020). Calcium silicate-based root canal sealers: a literature review. *Restorative Dentistry & Endodontics*. 45(3), e35. <https://doi.org/10.5395/rde.2020.45.e35>
- National Cancer Institute. (2011). EDTA. National Cancer Institute at the National Institutes of Health [Internet]. 2 Feb. 2011 [cited 2025 May 21]. Available from: <https://www.cancer.gov/publications/dictionaries/cancer-terms/def/edta>
- National Center for Biotechnology Information. "Calcium Metasilicate." PubChem, U.S. National Library of Medicine, <https://pubchem.ncbi.nlm.nih.gov/compound/Calcium-metasilicate>.
- Nguyen, G.N., Rothstein, S.J., Spangenberg, G. and Kant, S. (2015). Role of microRNAs involved in plant response to nitrogen and phosphorous limiting conditions. *Frontiers in Plant Science*. 6, 629. <https://doi.org/10.3389/fpls.2015.00629>
- Norwich, K.H. (2010). Le Chatelier's principle in sensation and perception: fractal-like enfolding at different scales. *Frontiers in Physiology*. 1, 17. <https://doi.org/10.3389/fphys.2010.00017>
- PubChem. (2025). Calcium Citrate. PubChem [Internet]. National Institutes of Health. [cited 2025 Apr 14]. Available from: <https://pubchem.ncbi.nlm.nih.gov/compound/Calcium-citrate#section=Physical-Description>
- Rinsi, B. and Espen, L. (2015). Mineral nitrogen sources differently affect root glutamine synthetase isoforms and amino acid balance among organs in maize. *BMC Plant Biology*. 15, 96. <https://doi.org/10.1186/s12870-015-0482-9>
- Schka, E. and Sadowski, G. (2024). Rigorous modeling the pH-dependent solubility of weak acids, weak bases and their salts. *Fluid Phase Equilibria*. 580, 114039. <https://doi.org/10.1016/j.fluid.2024.114039>
- Sketchfab. Crystal structure of wollastonite (ortho) [Internet]. Sketchfab; 2021 [cited 2025 Apr 15]. Available from: <https://sketchfab.com/3d-models/crystal-structure-of-wollastonite-ortho-cfce6c32d0824ab0b7c450c54fc1b5d4>
- The Protein Man. (2014). Biological buffers: pH range and how to prepare them. Gbiosciences.com [Internet]. [cited 2025 Apr 14]. Available from: <https://info.gbiosciences.com/blog/bid/197554/biological-buffers-ph-range-and-how-to-prepare-them>
- Wei, L., Chen, C. and Xu, Z. (2010). Citric acid enhances the mobilization of organic phosphorus in subtropical and tropical forest soils. *Biology and Fertility of Soils*. 46, [no page range provided]. <https://doi.org/10.1007/s00374-010-0464-x>
- Weller MT, Overton T, Rourke J, Armstrong F. *Inorganic chemistry*. 7th ed. Oxford: Oxford University Press; 2018.
- Wypych G. *Handbook of Fillers*. Elsevier; 2021.

